NFATc1 affects mouse splenic B cell function by controlling the calcineurin–NFAT signaling network

Sankar Bhattacharyya,[1] Jolly Deb,[1] Amiya K. Patra,[1] Duong Anh Thuy Pham,[1] Wen Chen,[1] Martin Vaeth,[1] Friederike Berberich-Siebelt,[1] Stefan Klein-Hessling,[1] Edward D. Lamperti,[3] Kurt Reifenberg,[4] Julia Jellusova,[5] Astrid Schweizer,[5] Lars Nitschke,[5] Ellen Leich,[2] Andreas Rosenwald,[2] Cornelia Brunner,[6] Swen Engelmann,[7] Ursula Bommhardt,[7] Andris Avots,[1] Martin R. Müller,[3] Eisaku Kondo,[8] and Edgar Serfling[1]

[1]Department of Molecular Pathology, [2]Institute of Pathology, University of Würzburg, D-97080 Würzburg, Germany
[3]Immune Disease Institute and Harvard Medical School, Boston, MA 02114
[4]Central Animal Facility, University of Mainz, D-55101 Mainz, Germany
[5]Department of Genetics, University of Erlangen-Nürnberg, D-91058 Erlangen, Germany
[6]Department of Physiological Chemistry, University of Ulm, D-89081 Ulm, Germany
[7]Institute of Medical and Clinical Immunology, University Magdeburg, D-39120 Magdeburg, Germany
[8]Department of Pathology, Okayama University Graduate School of Medicine, Dentistry, and Pharmaceutical Sciences, Okayama 700-8558, Japan

By studying mice in which the *Nfatc1* gene was inactivated in bone marrow, spleen, or germinal center B cells, we show that NFATc1 supports the proliferation and suppresses the activation-induced cell death of splenic B cells upon B cell receptor (BCR) stimulation. BCR triggering leads to expression of NFATc1/αA, a short isoform of NFATc1, in splenic B cells. NFATc1 ablation impaired Ig class switch to IgG3 induced by T cell–independent type II antigens, as well as IgG3$^+$ plasmablast formation. Mice bearing NFATc1$^{-/-}$ B cells harbor twofold more interleukin 10–producing B cells. NFATc1$^{-/-}$ B cells suppress the synthesis of interferon-γ by T cells in vitro, and these mice exhibit a mild clinical course of experimental autoimmune encephalomyelitis. In large part, the defective functions of NFATc1$^{-/-}$ B cells are caused by decreased BCR-induced Ca^{2+} flux and calcineurin (Cn) activation. By affecting CD22, Rcan1, CnA, and NFATc1/αA expression, NFATc1 controls the Ca^{2+}-dependent Cn–NFAT signaling network and, thereby, the fate of splenic B cells upon BCR stimulation.

CORRESPONDENCE
Edgar Serfling:
serfling.e@
mail.uni-wuerzburg.de

Abbreviations used: AICD, activation-induced cell death; BAC, bacterial artificial chromosome; Btk, Bruton's tyrosine kinase; ChIP, chromatin immunoprecipitation; Cn, calcineurin; CsA, cyclosporin A; EAE, experimental autoimmune encephalomyelitis; GC, germinal center; IP_3, inositol 1,4,5-triphosphate; MZB, marginal zone B cell; PI, propidium iodide; PLC-γ2, phospholipase Cγ2; TD, T cell dependent; TI, T cell independent; T+I, TPA (12-O-tetradecanoylphorbol-13-acetate)+ ionomycin.

The survival of mature peripheral lymphocytes is controlled by their immune receptors. In cascades of molecular events, extracellular signals are transmitted through immune receptors to transcription factors that orchestrate the expression of batteries of genes, and thus such fundamental processes as the activation, proliferation, and elimination of lymphoid cells. For resting peripheral B lymphocytes, "tonic" B cell receptor (BCR) signals have been described as essential for survival. Ablation of BCR surface expression or inhibition of BCR signaling led to the death of resting mature B cells within 3–6 d (Lam et al., 1997; Kraus et al., 2004). However, mature B cells lacking a BCR could be rescued by the ectopic expression of a constitutive active version of P110α, a catalytic subunit of PI3 kinase. These and further findings indicated the PI3 kinase–protein kinase B (Akt) signaling cascade as a signaling pathway that supports the survival of resting mature B

S. Bhattacharyya, J. Deb, and A.K. Patra contributed equally to this paper.
M. R. Müller's present address is Dept. of Haematology, Oncology and Immunology, University of Tübingen, 72076 Tübingen, Germany.
E. Kondo's present address is Division of Oncological Pathology, Aichi Cancer Center Research Institute, Nagoya 464-8681, Japan.

The Rockefeller University Press $30.00
J. Exp. Med. Vol. 208 No. 4 823-839
www.jem.org/cgi/doi/10.1084/jem.20100945

cells by tonic BCR signals in the periphery (Srinivasan et al., 2009). Although these and other studies elucidated important signaling molecules for the survival of resting peripheral B cells, they did not address which signaling pathways control the survival and function of peripheral B cells upon BCR stimulation.

In a typical immune response, triggering of immune receptors by cognate antigens culminates in the massive clonal expansion of peripheral lymphocytes, followed by elimination of most of the amplified effector cells by apoptosis toward the end of the immune response (Strasser and Pellegrini, 2004; Krammer et al., 2007). Although immune reactions depend on numerous parameters, immune receptor signals are key determinants that control the strength of an immune response and the onset of apoptosis, and thus the termination of the immune response. Triggering of BCR results in the rapid phosphorylation of several proximal signaling molecules, such as Bruton's tyrosine kinase (Btk), phospholipase Cγ2 (PLC-γ2), and others, by the tyrosine protein kinases Lyn and Syk. Along with tyrosine phosphorylated B cell adaptor proteins, such as SLP-65/BLNK, these molecules assemble in supramolecular complexes that transmit BCR signals to downstream serine/threonine protein kinases and, finally, to transcription factors. By hydrolyzing phosphatidylinositols to diacylglycerol and inositol 1,4,5-triphosphate (IP_3) that, in turn, binds to and stimulates IP_3 receptors, PLC-γ2 affects the release of Ca^{2+} from intracellular stores and the subsequent influx of extracellular Ca^{2+} (King and Freedman, 2009). An increase in intracellular Ca^{2+} levels leads to the activation of the Ca^{2+}/calmodulin-dependent Ser/Thr-specific phosphatase calcineurin (Cn; also designated as PP2B), which dephosphorylates and activates members of NFAT transcription factors by facilitating their nuclear translocation.

Together with NFATc2 (also designated as NFAT1), NFATc1 (or designated as NFAT2) belongs to the most prominent NFAT factors in activated lymphocytes. However, contrary to NFATc2, which is constitutively expressed in most peripheral lymphocytes, the expression of NFATc1 in peripheral lymphocytes is strongly induced at the transcriptional level. In $CD4^+$ T cells, the transcription of *Nfatc1* gene is induced by TCR triggering and co-stimulatory signals (Chuvpilo et al., 1999, 2002; Nurieva et al., 2007), whereas, as we show here, BCR triggering induces NFATc1 expression in splenic B cells. The induction of NFATc1 expression upon immune receptor stimulation is an important control level of NFAT activity. The observation that NFAT factors have to reach a certain threshold level for the induction of the IL-2 (*Il2*) promoter in T cells was made nearly 20 yr ago (Fiering et al., 1990). The induction of *Nfatc1* gene is controlled by a switch from the constitutively active promoter P2 to the inducible P1 promoter, whose activity directs the predominant synthesis of short isoform NFATc1/αA (Chuvpilo et al., 2002). This isoform differs from other NFATc proteins in its short C terminus, and thus lacks a second transactivation domain present in longer NFATc1 isoforms (Avots et al., 1999) that harbor two highly conserved sumoylation motifs (Nayak et al., 2009). NFATc1/αA contains an individual N-terminal peptide, designated as α-peptide, which differs markedly from that in NFATc2 and other NFATc proteins, including the NFATc1/β isoforms (Serfling et al., 2006). Although the functional relevance of these protein domains remains to be shown in detail, it is very likely that along with its high expression level, NFATc1/αA exerts specific functions in T cell and B cell physiology.

NFAT factors were originally described as regulators of cytokine genes in T cells, such as of Il2, Il3, Il4, Il5, *Ifng*, and *Tnf*α genes (Serfling et al., 2000; Hogan et al., 2003; Macian, 2005), but they also orchestrate the expression of numerous other genes in other cells, including B cells. However, apart from a study on the inactivation of Cn B1 subunit (Winslow et al., 2006), which affects all NFATc members and probably more downstream effectors, there is only a restricted number of comprehensive analyses on NFAT function in B cells. Investigations of B cell differentiation in mice bearing $NFATc1^{-/-}$ lymphocytes upon reconstitution of RAG-deficient mice with *Nfatc1*$^{-/-}$ fetal liver cells indicated a crucial role for NFATc1 in the development of peritoneal B1a cells (Berland and Wortis, 2003). In mice created by complementation of $RAG^{-/-}$ blastocysts with *Nfatc1*$^{-/-}$ embryonic stem cells, a strong decrease in α-IgM–mediated proliferation of $NFATc1^{-/-}$ B cells was observed (Yoshida et al., 1998).

By using mice in which the *Nfatc1* gene was inactivated in BM, spleen, or germinal center (GC) B cells, we show that NFATc1 controls the fate of splenic B cells upon BCR stimulation. NFATc1 inactivation impaired BCR-mediated proliferation and facilitated activation-induced cell death (AICD). Although, apart from the loss of peritoneal B1a cells, NFATc1 ablation did not markedly affect B cell differentiation in BM and periphery, it resulted in a strong decrease of Ig class switch to IgG3 upon immunization with T cell–independent type II antigens and $IgG3^+$ plasmablast formation. NFATc1 ablation also resulted in a decreased capacity of $NFATc1^{-/-}$ B cells to stimulate T cells to proliferate and to secrete IL-2 and IFN-γ in vitro. This is caused in part by an increase in IL-10–producing $CD1d^{high}CD5^+$ B cells, which might also contribute to the mild clinical course of experimental autoimmune encephalomyelitis (EAE) in mice bearing $NFATc1^{-/-}$ B cells in vivo. Several of these defects seem to depend on intracellular Ca^{2+} levels, which were found to be decreased in $NFATc1^{-/-}$ splenic B cells. In this study, we show that, in addition to NFATc1/αA induction, NFATc1 regulates the expression and activity of further members of the Ca^{2+}-dependent Cn network, such as CD22, Rcan1, CnA, and NFATc2, and thus affects the survival and function of peripheral B cells.

RESULTS

BCR triggering of naive splenic B cells leads to strong induction of NFATc1/αA

Stimulation of naive splenic B cells from 6–8-wk-old mice with 10 μg/ml anti-IgM antibody (α-IgM; the $F(ab')_2$ fragment of anti–mouse IgM) in vitro leads to strong induction of NFATc1 after ∼24 h. A similar strong induction of NFATc1 was also detected by TPA+ionomycin (T+I) treatment,

whereas a much weaker induction was observed after stimulation of B cells with 10 µg/ml LPS or 2 µg/ml α-CD40 (Fig. 1 A and Fig. S1 A). The short NFATc1 protein induced by α-IgM reacted with an antibody raised against the NFATc1 α-peptide and corresponds to NFATc1/αA, whereas the NFATc1 version induced by LPS did not react (Fig. 1 B). The Western blot data on the important role of BCR signals in NFATc1 induction are supported by the strong induction of an *Egfp* reporter gene controlled by the *Nfatc1* locus upon α-IgM stimulation. When splenic B cells from mice bearing a BAC-*Nfatc1/Egfp* transgene were stimulated by α-IgM, LPS, or α-CD40 for 24 h, a much stronger GFP induction was detected after α-IgM than after LPS or α-CD40 treatment (Fig. 1 C).

To show that BCR-mediated induction of NFATc1 is affected by prototypical signaling molecules of the BCR-signaling pathways, we investigated the effect of α-IgM stimulation on NFATc1 induction in splenic B cells from mice deficient for the protein tyrosine kinase Btk (Kerner et al., 1995; Khan et al., 1995) or the adaptor molecule SLP-65 (Jumaa et al., 1999). As shown in Fig. 1 (D and E), inactivation of either Btk or SLP-65 led to complete loss of NFATc1 induction, indicating that the strong induction of NFATc1/αA is mediated through these signaling molecules, which are known to be key components of BCR signaling.

NFATc1 ablation suppresses the formation of peritoneal B1a cells, but does not interfere with B cell development in BM and spleen

To investigate the role of NFATc1 in B cell physiology we used mice bearing "floxed" exon 3 alleles of *Nfatc1* (*Nfatc1*$^{flx/flx}$). To generate mice in which the murine *Nfatc1* gene was inactivated in B cells, *Nfatc1*$^{flx/flx}$ mice were crossed with mice that specifically express the cre enzyme in B cells of BM (*mb1-cre*; Hobeika et al., 2006), spleen (*Cd23-cre*; Kwon et al., 2008), or GC (*Aicda-cre*; Kwon et al., 2008). Crossing of *Nfatc1*$^{flx/flx}$ mice with the *mb1-cre* and *Cd23-cre* lines resulted in the ablation of NFATc1 expression in splenic B cells (Fig. S1, B–D).

Flow cytometric analyses of B cell development in BM from WT and *mb1-cre* x *Nfatc1*$^{flx/flx}$ mice did not show significant differences in the expression of B220, CD43, BP-1, CD24, IgM, and IgD on pro–B cells (Hardy fractions B and C; Hardy and Hayakawa, 2001; CD24^{+}BP-1^{-} and CD24^{+}BP-1^{+} fractions in B220^{+}CD43^{hi} cells), pre–B cells, and immature and mature B cells (Hardy fractions D–F; Hardy and Hayakawa, 2001; Fig. S2 A). Likewise, the differentiation of LN and splenic NFATc1$^{-/-}$ B cells appeared to be relatively unaffected (Fig. S2 B), although only 75–80% B cells were counted in preparations of whole splenic B cells from 7 *mb1-cre* x *Nfatc1*$^{flx/flx}$ mice compared with WT mice. Stains of splenic B cells for CD21+CD23 revealed similar ratios of follicular B cells and marginal zone B cells (MZBs) from WT and *mb1-cre* x *Nfatc1*$^{flx/flx}$ mice (Fig. S2 C). Also, the maturation of splenic B cells did not markedly differ between WT and NFATc1$^{-/-}$ cells (Fig. S2 D). However, in agreement with published data (Berland and Wortis, 2003), in peritoneal washes from *mb1-cre* x *Nfatc1*$^{flx/flx}$ mice a 5–10-fold decrease in the population of B1a cells was detected. In the peritoneum of *Cd23-cre* x *Nfatc1*$^{flx/flx}$ mice, B1a cells that do not express CD23 were found in normal numbers (Fig. S2, E and F).

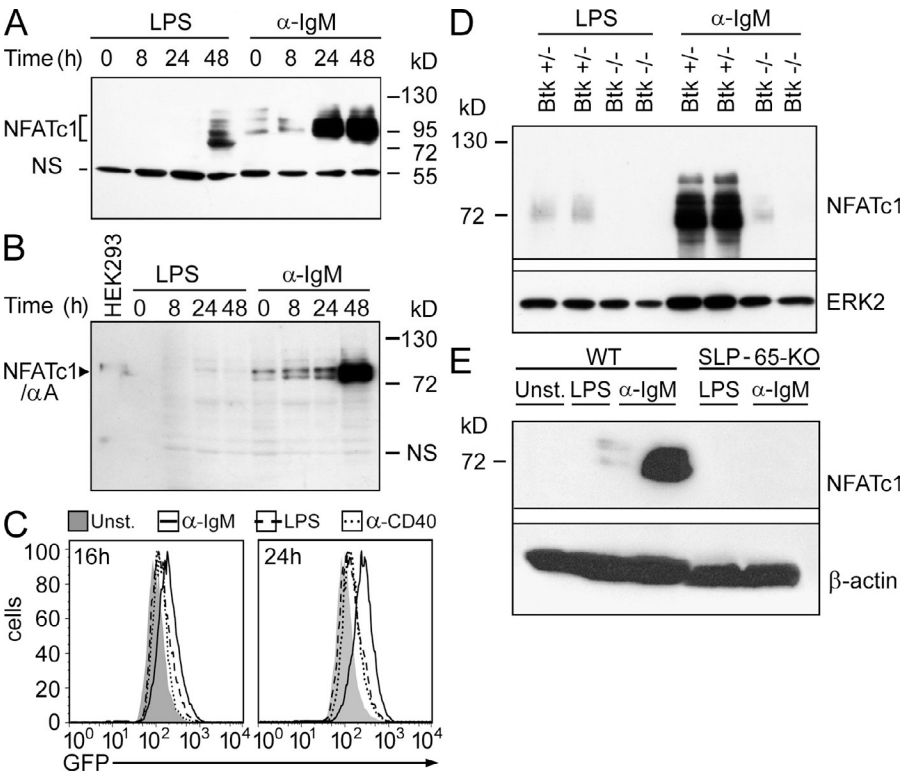

Figure 1. NFATc1 induction in naive mouse splenic B cells. (A and B) Freshly prepared splenic B cells were stimulated with 10 µg/ml α-IgM or 10 µg/ml LPS for 0–48 h. Whole-cell protein was fractionated on 8% polyacrylamide gels and immunoblotted with either the mAb 7A6 recognizing all NFATc1 isoforms (A) or an antibody raised against the N-terminal α-peptide of NFATc1 (B). In lane 1 of panel B, protein from HEK 293 cells transfected with an NFATc1/αA expression plasmid was fractionated. NS, nonspecific band. (C) Splenic B cells from mice expressing an *Nfatc1-Egfp* reporter transgene were either left unstimulated or stimulated for 16 or 24 h. GFP fluorescence was determined by flow cytometry. (D and E) Splenic B cells from WT, Btk-deficient, or SLP-65-deficient mice were left unstimulated (Unst.) or were stimulated with LPS or α-IgM for 24 h, and whole protein extracts were immunoblotted using the NFATc1-specific mAb 7A6. ERK2 and β-actin, loading controls. In A-C, one typical experiment from more than three assays is shown; in D and E, one blot from two similar blots is presented.

Impaired BCR-induced proliferation and increased AICD of NFATc1$^{-/-}$ splenic B cells

Investigations of the α-IgM–mediated proliferative capacity of splenic NFATc1$^{-/-}$ B cells in CFSE dilution assays and [^{3}H]thymidine incorporation experiments showed a marked decrease in their proliferation in vitro, compared with WT B cells. In contrast, no differences in proliferation were observed between NFATc1$^{-/-}$ and WT B cells upon LPS or α-CD40 stimulation (Fig. 2 A and Fig. S3 A). In addition, NFATc1$^{-/-}$ splenic B cells showed a distinct increase in α-IgM–mediated apoptosis. This is reflected in the relative drop of living cells (as shown by their SSC-FSC features; Fig. S3 B) and the increase of Annexin V–positive apoptotic NFATc1$^{-/-}$ cells compared with WT B cells (Fig. 2 B). Similar differences in survival between WT and NFATc1$^{-/-}$ B cells were detected in cell cycle analysis by PI staining upon α-IgM stimulation for 48 h, showing a pronounced increase in hypoploid sub-G1 cells from ∼20–40% (Fig. S3 C). The increase in α-IgM–mediated AICD is a specific feature of NFATc1$^{-/-}$ B cells because contrary to those, NFATc2$^{-/-}$ B cells were resistant to α-IgM–mediated apoptosis (Fig. 2 B), which agrees with the pro-apoptotic activity of NFATc2 in activated T cells, as previously described (Chuvpilo et al., 2002).

NFATc1 controls numerous genes that affect the AICD of B cells

For the identification of NFATc1 target genes that control the proliferation and/or AICD of B cells, we investigated gene expression of splenic B cells by using mouse whole-genome expression arrays. Freshly isolated B cells from WT and *mb1-cre* x *Nfatc1*$^{flx/flx}$ mice were either left uninduced or induced by α-IgM for 3, 8, or 16 h. We identified 53 genes whose expressions were enhanced by more than twofold and 37 genes whose expression was suppressed more than twofold by NFATc1 upon α-IgM stimulation for 16 h (Tables S1 and S2). Among the enhanced "top ten" genes are the *Spp1*, *Rcan1*, *Pdcd1*, *Tnfsf14*, and *Fasl* genes that encode apoptosis regulators (Fig. 2 C). The *Spp1* gene encodes the multifunctional protein osteopontin (Hur et al., 2007); the *Rcan1* gene encodes the Cn modulator calcipressin (Vega et al., 2003); the *Pdcd1* gene encodes PD-1 (CD279), a member of the Ig supergene family which is expressed on T and B cells (Keir et al., 2008); and the *Tnfsf14* gene encodes LIGHT (CD258), a member of the TNF family that is a ligand of the lymphotoxin β receptor (LTβR) and herpes virus entry mediator (HVEM; Scheu et al., 2002). Although the RNA levels of all five genes were almost undetectable in nonstimulated B cells, the expression of *Spp1* and *Rcan1* genes was rapidly induced by α-IgM treatment for 3 h and decreased (*Spp1*) or remained quite constant (*Rcan1*) afterward in NFATc1$^{-/-}$, but not WT B cells. In contrast, the expression of *Pdcd1*, *Tnfsf14*, and *Fasl* genes was undetectable upon 3 h induction and increased strongly after 16 h of α-IgM stimulation in WT but not NFATc1$^{-/-}$ cells (Fig. 2 D).

To show that the *Spp1*, *Rcan1*, *Pdcd1*, *Tnfsf14*, and *Fasl* genes are genuine NFATc1 targets in splenic B cells, we performed chromatin immunoprecipitation (ChIP) assays using splenocytes that were either left noninduced or induced with T+I or α-IgM for 16 h. Upon immunoprecipitation with an NFATc1-specific antibody, we detected a marked increase in NFATc1 binding to the promoters of *Pdcd1*, *Tnfsf14*, and *Fasl* genes after both stimulations (Fig. 2 E). In contrast, the *Spp1* and *Rcan1* promoters already showed NFATc1 binding in nonstimulated cells, but stimulation increased their NFATc1 binding. As expected, for the *Il2* promoter an increase in NFATc1 binding was observed upon T+I stimulation but not upon α-IgM stimulation (Fig. 2 E).

To show whether in our assays PD-1 and LIGHT might affect the survival of B cells, we stimulated splenic B cells from PD-1 and LIGHT deficient mice by α-IgM. Compared with WT B cells, both types of B cells showed a strong reduction in AICD (Fig. S3 D). This indicates that three of the most prominent NFATc1 targets in primary B cells, the *Pdcd1, Tnfs14 and Fasl* genes, code for proapoptotic proteins.

Apart from the *Ccnb1*/Cyclin B1 gene, among the 53 genes that showed a twofold and stronger increase in expression upon BCR stimulation in WT (compared with NFATc1$^{-/-}$ B cells) we did not detect genes that directly control cell cycle and proliferation (Table S1). This suggests that NFATc1 enhances the expression of (numerous) genes controlling proliferation only to moderate levels. Such view finds support in gene set enrichment analyses (GSEA) of microarray data in which numerous gene signatures enhancing proliferation were significantly enriched in WT B cells compared with NFATc1$^{-/-}$ B cells. Among those are eleven signatures that are significantly associated with cell cycle and proliferation (Table I), and numerous cell cycle–associated genes. In addition to the *Ccnb1* gene, these include several cyclin genes, which are listed as signature genes in leading edge analyses (Table S3).

NFATc1 supports the proliferation of B cells by controlling their Ca^{2+} flux and Cn activity

Among the 10 genes whose expression was most strongly suppressed by NFATc1 in B cells are the *Cd22*, *Fcer2a*/CD23, and *S100a4* genes, whose activity modulates (or is modulated by) intracellular Ca^{2+} levels in B cells (Fig. 3 A; Kolb et al., 1990; Nitschke, 2009; Matsuura et al., 2010). These findings suggest that NFATc1, as one of the most prominent NFATc1 targets (along with Rcan1; Figs. 2, C and E), controls BCR-mediated, store-operated Ca^{2+} entry, and thus the Ca^{2+}-dependent Cn network, for its own induction in B cells.

Sustained Ca^{2+} entry is necessary for many physiological processes controlling lymphocyte activity, including their proliferation and apoptosis (Hogan et al., 2010). This is illustrated for splenic B cells in Fig. 3 B. Almost all cells proliferated when freshly prepared splenic B cells were cultured in X-vivo medium, a medium rich in Ca^{2+}, whereas in a 1:1 mixture of X-vivo and RPMI media (the latter contains about one-third the amount of Ca^{2+} as the X-vivo medium) <50% of B cells were found to proliferate. Adding 10 mM Ca^{2+} to this medium restored the proliferative capacity, whereas inhibiting Cn by cyclosporin A (CsA), either at the start of

the experiment or 1 d later, blocked any proliferation of B cells (Fig. 3 B). A similar strong effect has been observed with 10 µM NCI3, a novel Cn inhibitor (Sieber et al., 2007), and 2.5-µM Vivit-11R (Fig. S4, A and C), a specific NFAT inhibitor (Aramburu et al., 1999). The mild proliferative defect of NFATc1$^{-/-}$ B cells upon α-IgM stimulation (Fig. 2 A and Fig. 3 B) is in line with the observation that NFATc1$^{-/-}$ B cells exhibit a marked reduction in Ca^{2+} flux (Fig. S4 E),

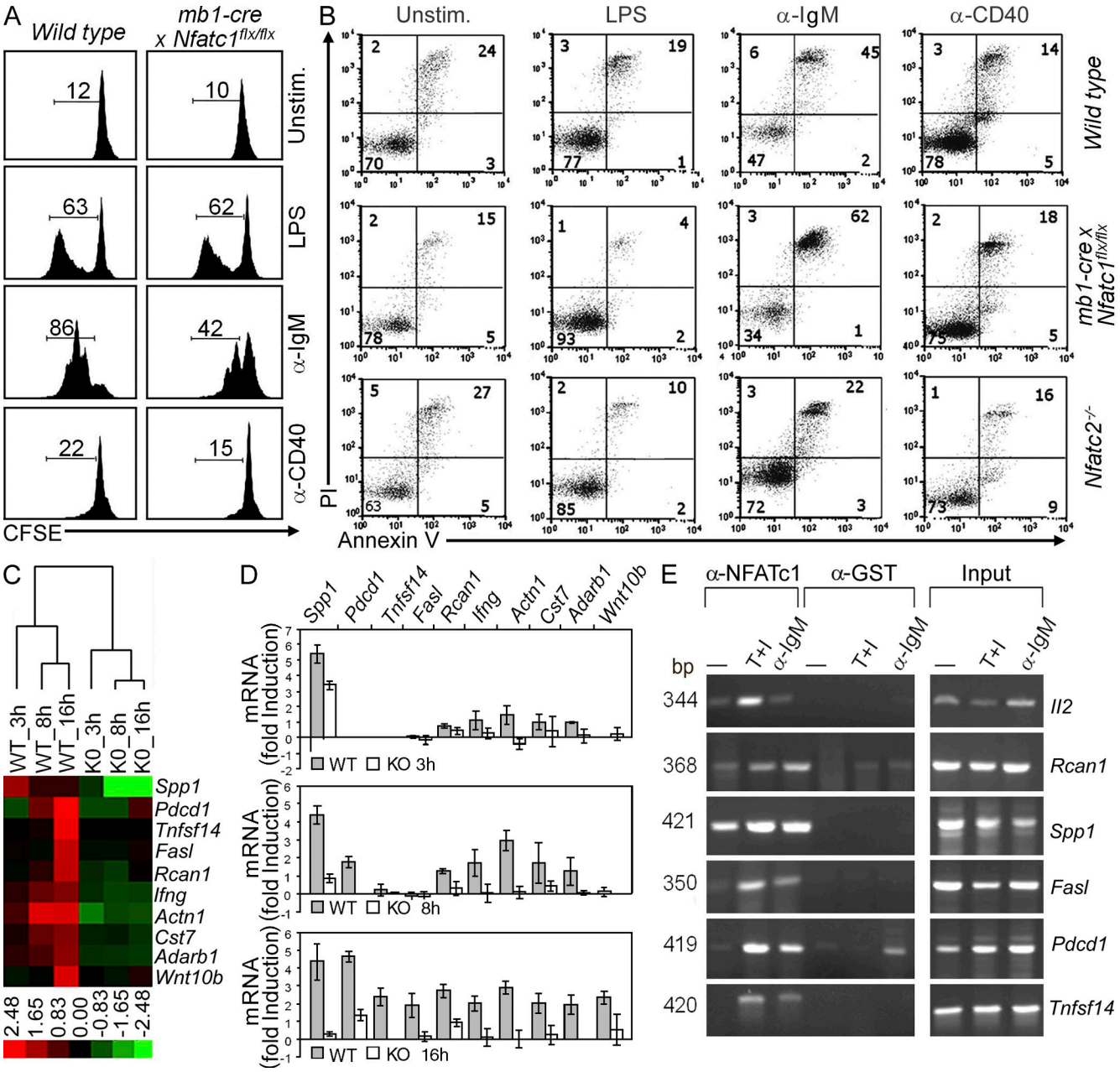

Figure 2. NFATc1 is required for optimal proliferation and survival of splenic B cells. (A) CFSE-labeled splenic B cells from a WT and *mb1-cre x Nfatc1*$^{flx/flx}$ mouse were incubated for 72 h in the absence (Unstim.) or presence of 10 µg/ml LPS, 10 µg/ml α-IgM, or 2 µg/ml α-CD40. CFSE dilution was measured by flow cytometry. (B) Splenic B cells from WT, *mb1-cre x Nfatc1*$^{flx/flx}$, and *Nfatc2*$^{-/-}$ mice were incubated for 72 h; cells were stained with PI and Annexin V and analyzed by flow cytometry. (C) WT and *mb1-cre x Nfatc1*$^{flx/flx}$ (KO) splenic B cells were stimulated with α-IgM, as indicated. Gene expression was analyzed by DNA microarray. Key at the bottom indicates the fold changes in gene expression (log_2 values). (D) Induction of 10 NFATc1 target genes by α-IgM stimulation in WT and NFATc1$^{-/-}$ splenic B cells. Error bars show ± the SEM. (E) ChIP assay showing the in vivo binding of NFATc1 in splenocytes to the promoters of *Il2*, *Rcan1*, *Spp1*, *Fasl*, *Pdcd1*, and *Tnfsf14* genes upon stimulation for 16 h with α-IgM or T+I. Lanes 1–3, ChIP assays using splenocytes that were left unstimulated (-) or stimulated by T+I or α-IgM for 16 h. ChIP assays were also performed using an antibody directed against GST protein. As input control, 1% of chromatin of all assays was used. In A and B, one typical experiment is shown from more than three assays; in C and D, mean values from three individual DNA microarray analyses are presented, and in E one typical ChIP assay from three assays is shown.

Table I. Gene set enrichment analysis

Pathways/ signatures	References	Enriched in WT	Enriched in *Nfatc1*$^{-/-}$ B cells	Nominal P value	FDRq value
Cell cycle	Brentani et al., 2003 Cho et al., 2001 Whitfield et al., 2002 Liu et al., 2004	Yes	No	<0.0001	<0.07
Proliferation	Shaffer et al., 2002 Rosenwald et al., 2002 Su et al., 2004	Yes	No	<0.0001	<0.09
Myc targets	Zeller et al., 2003 Yu et al., 2005	Yes	No	<0.01	<0.08
Antiapoptosis	Wu et al., 2002	Yes	No	≤0.01	<0.08
Wnt signaling	Kenny et al., 2005	Yes	No	<0.031	0.24

Gene set enrichment analysis (GSEA) of microarray data of splenic B cells from WT and *mb1-cre x Nfatc1*$^{fix/fix}$ mice stimulated for 16 h by α-IgM using 81 lymphoma-associated signatures from the signature database of the Staudt laboratory (http://lymphochip.nih.gov/signaturedb) and 1.687 curated gene sets (c2) from the Molecular Signatures Database (MSigDB; Subramanian et al., 2005). All references mentioned in Table I are cited in Subramanian et al., 2005.

in both the release of Ca^{2+} from intracellular stores and in influx of extracellular Ca^{2+} to ∼60% of level to that in WT cells (Fig. 3 C).

CD22 is an inhibitory co-receptor of BCR that is transiently expressed on splenic B2 cells (Nitschke, 2009). Its surface expression is impaired by BCR stimulation (Lajaunias et al., 2002) and, as flow cytometric assays of WT and NFATc1$^{-/-}$ B cells imply, NFATc1 contributes to CD22 suppression (Fig. 3 D). This conclusion is supported by the DNA microarray data (Fig. 3 A and Table S2) and semiquantitative RT-PCR assays that showed higher CD22 RNA levels in NFATc1$^{-/-}$ than WT B cells treated by α-IgM for 16 h (Fig. 3 D). Splenic B cells from CD22$^{-/-}$ mice show, on the other hand, a strong NFATc1/αA expression in noninduced and LPS-treated B cells, whereas WT B cells express isoforms other than NFATc1/αA under these conditions (Fig. 1 A and Fig. S4 F).

In addition to the *Rcan1* gene, the *Ppp3cb* gene encoding the large CnA β subunit that is predominantly expressed in lymphocytes is a further direct NFAT target. This has been shown previously for cardiomyocytes (Oka et al., 2005), and in ChIP assays we detected the in vivo binding of NFATc1 to the 5′ region of *Ppp3cb* gene upon α-IgM stimulation (Fig. 3 E, top), whereas no NFATc1 binding was found to the 5′ region of *Ppp3ca* gene (not depicted). In Western blots using an antibody recognizing CnA α/β proteins, a strong decrease in the α-IgM–mediated induction of one CnA-specific protein was detected in protein extracts from NFATc1$^{-/-}$ B cells (Fig. 3 E, middle), suggesting an important role of NFATc1 in CnA expression and function. This conclusion is supported by the marked decrease of Cn activity in extracts from freshly prepared NFATc1$^{-/-}$ B cells, compared with WT B cells (Fig. 3 E, bottom).

The diminished Cn activity suggests that the activation of other NFATc factors might also be impaired in NFATc1$^{-/-}$ B cells. In immunohistochemical stainings of B cells from WT and *mb1-cre x NFATc1*$^{flx/flx}$ mice stimulated for 1 or 2 d with α-IgM and α-CD40 and restimulated for 30 min with T+I, we detected markedly less NFATc2 in nuclei of NFATc1$^{-/-}$ B cells than WT cells (Fig. 3 F). This suggests an impaired NFATc2 activation in the absence of NFATc1. In RNA levels, no differences were detected for NFATc2 RNA between WT and NFATc1$^{-/-}$ B cells, whereas a slight decrease in NFATc3 RNA levels was observed for NFATc1$^{-/-}$ B cells, compared with WT cells (Fig. 3 F). However, because no distinct increase in NFATc3 RNA levels was detected upon α-IgM stimulation in WT B cells (Fig. 3 F), NFATc1 appears to indirectly affect *Nfatc3* gene expression.

Collectively, these data indicate that NFATc1 controls Rcan1 and CnA expression, i.e., its immediate upstream control molecules, which, in a feedback loop, affect the transcriptional induction of NFATc1. In addition, NFATc1 seems to also affect upstream BCR signals, probably through CD22 and other targets. A scheme of this network connecting NFATc1 with its upstream activators in B cells is shown in Fig. S5A.

NFATc1 affects Ig class switch by T cell–independent type II antigens

Interruption of BCR signaling by inactivating Btk, SLP-65, PLC-γ2, and further components of the BCR signaling cascade not only leads to a drastic decrease in Ca^{2+} flux, but also to defects in Ig class switching upon immunization with T cell–independent type II (TI-II) antigens (Kerner et al., 1995; Khan et al., 1995; Jumaa et al., 1999; Wang et al., 2000). When we measured Ig levels in sera from nonimmunized WT mice and mice bearing NFATc1$^{-/-}$ B cells, we did not detect statistically significant differences in the concentration of Ig classes (except IgM in *Cd23-cre x Nfatc1*$^{flx/flx}$ mice; Fig. S5 B). However, upon immunization with the TI-II antigen NP-Ficoll, we detected 10-fold lower IgG3 serum levels in *Cd23-cre x Nfatc1*$^{flx/flx}$ mice, compared with those from WT mice. Slight, but statistically significant, differences were also detected in IgM levels 2 wk after immunization (Fig. 4 A). Very similar results were obtained upon immunization of *Aicda-cre x Nfatc1*$^{flx/flx}$ mice that resulted in tenfold lower IgG3 serum levels compared

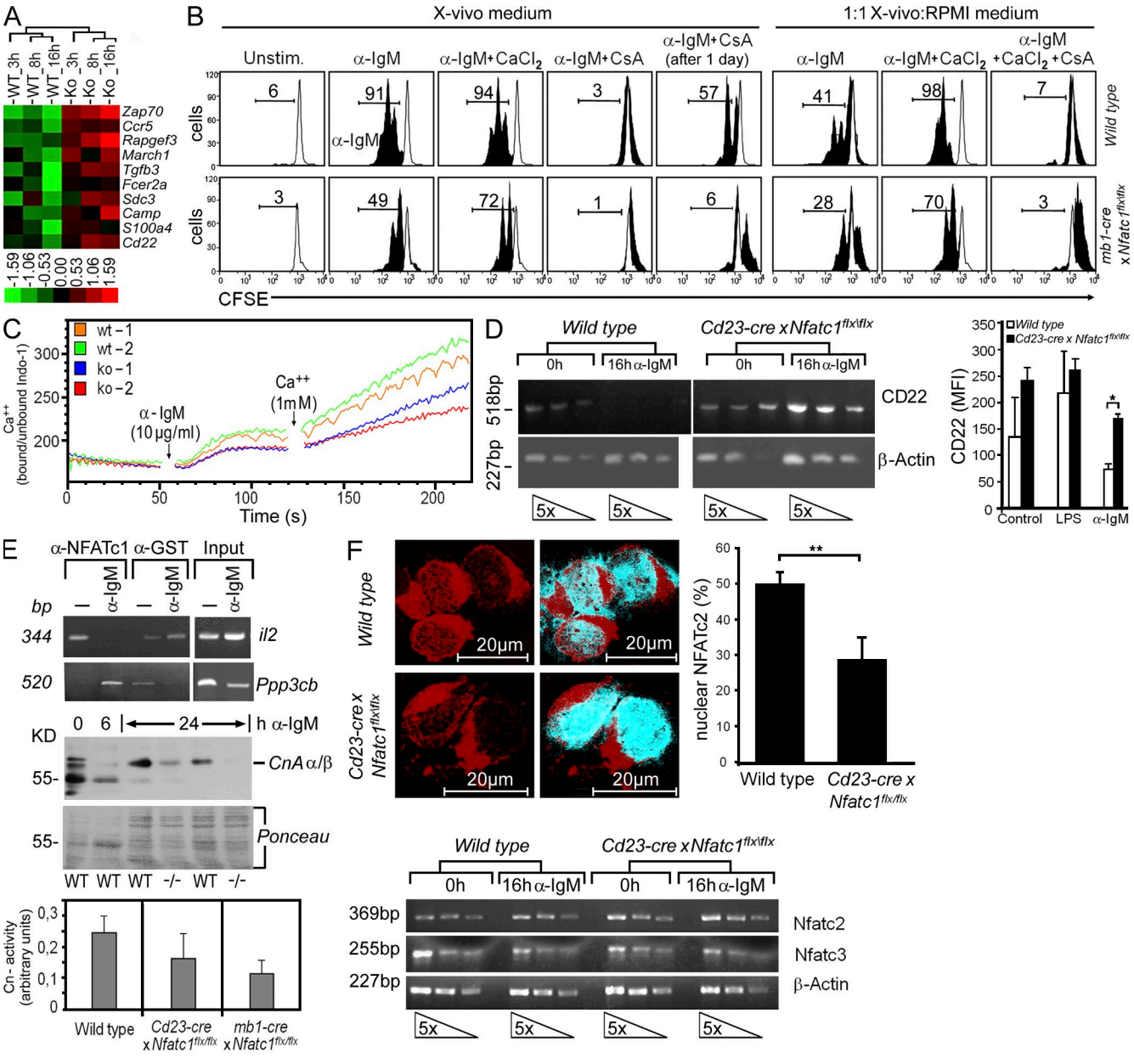

Figure 3. NFATc1 controls Ca^{2+}/Cn signaling in splenic B cells. (A) DNA microarray assay showing 10 genes whose expression was enhanced in B cells from *mb1-cre x Nfatc1$^{flx/flx}$* mice compared with WT B cells. Mean values of 3 individual assays are shown. (B) Manipulation of Ca^{2+}/Cn signaling by adding 10 mM $CaCl_2$ or 100 ng/ml CsA to proliferation assays. Splenic B cells from WT or *mb1-cre x Nfatc1$^{flx/flx}$* mice were stained with CFSE and treated with 10 μg/ml α-IgM in the absence or presence of Ca^{2+} or CsA in X-vivo medium or 1:1 X-vivo+RPMI medium that contains less Ca^{2+}. Numbers indicate the percentage of cycling cells. One typical set of more than three experiments is shown. (C) Ca^{2+} release and influx in B cells from WT and *mb1-cre x Nfatc1$^{flx/flx}$* (KO) mice. One typical experiment from more than three assays is shown. (D) Effect of NFATc1 ablation on CD22 expression. (left) Semiquantitative RT-PCR assay showing an increase in CD22 RNA in NFATc1$^{-/-}$ splenic B cells. One typical assay from three individual assays is shown. (right) Flow cytometric detection of CD22 expression on WT and *Cd23-cre x Nfatc1$^{flx/flx}$* splenic B cells left unstimulated or stimulated with LPS or α-IgM for 2 h. Two more assays with B cells from two mice each were performed and gave similar results. (E) CnA assays. (top) ChIP assay for the binding of NFATc1 to the *Ppp3cb* and *Il2* promoter in vivo. Splenocytes were left unstimulated (−) or stimulated with α-IgM for 16 h. As indicated, either an NFATc1-specific or an unrelated antibody (α-GST) was used. As input control, 1% of chromatin of all assays was used. (middle) Immunoblot using whole cellular protein from B cells and a CnA α/β-specific antibody. Below the blot, Ponceau red staining is shown as loading control. (bottom) Mean values of Cn activity from three assays are shown ($P \geq 0.05$ between WT and *mb1-cre x Nfatc1$^{flx/flx}$* cells). (F) Effect of NFATc1 ablation on NFATc2 expression. (top) Decrease in nuclear NFATc2 in NFATc1$^{-/-}$ B cells. Splenic B cells were treated with α-IgM and α-CD40 for 24 h, and for the last 30 min, the cells were also treated with T+I. Splenic B cells stained with an NFATc2-specific antibody. (right) Nuclear staining of 100 cells measured by confocal microscopy is compiled. (bottom) Semiquantitative RT-PCR assay. Error bars show ± the SEM.

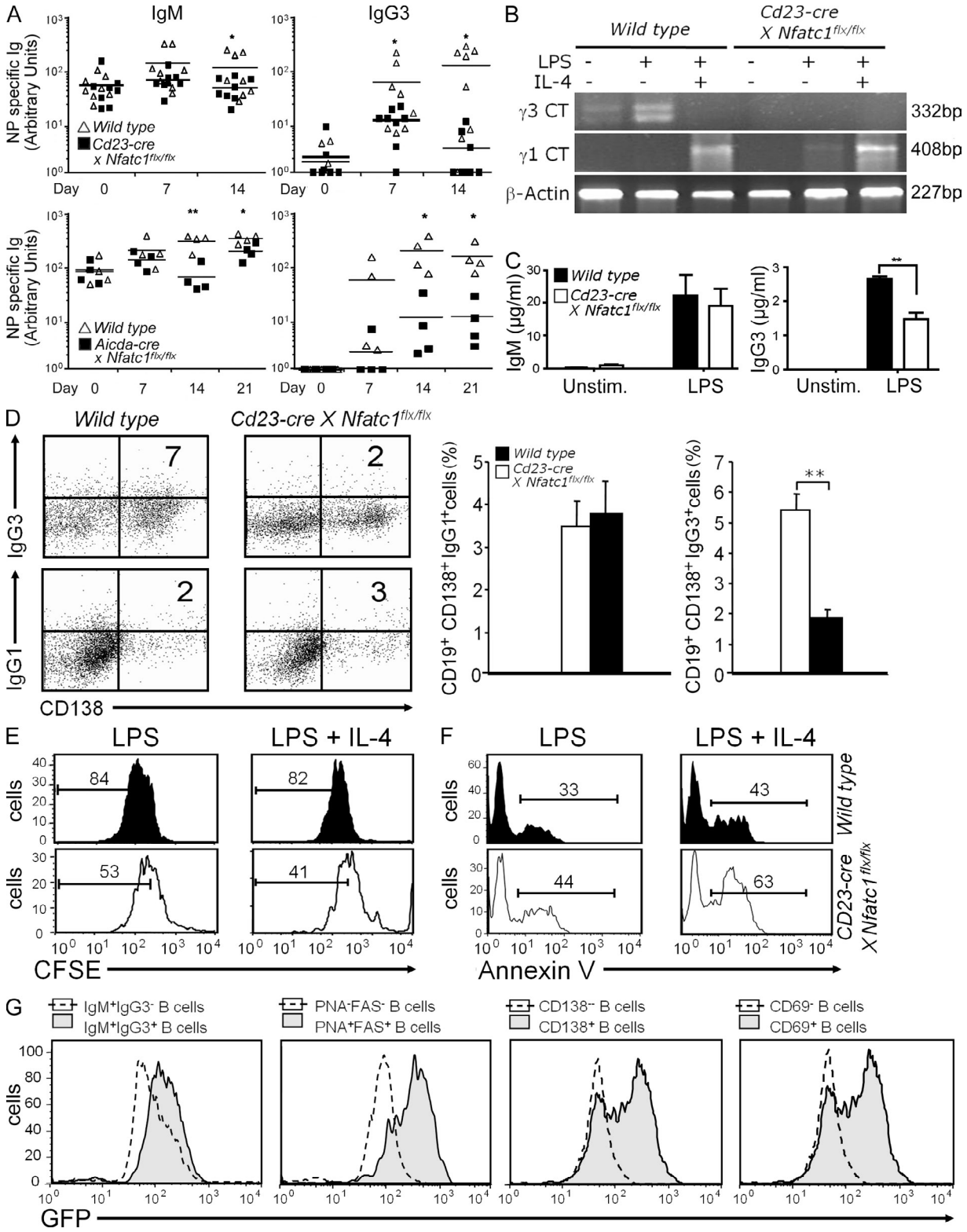

Figure 4. NFATc1 deficiency results in a defect in IgG3 class switch by the TI-type II antigen NP-Ficoll. (A) IgM and IgG3 levels in sera of WT, *Cd23-cre*, and *Aicda-cre x Nfatc1*$^{flx/flx}$ mice after immunization with the TI-type II antigen NP-Ficoll. Each symbol represents one mouse. (B) Appearance of circular IgG3 and IgG1 transcripts in WT and NFATc1$^{-/-}$ splenic B cells after in vitro culture for 2 d in the presence of LPS. (C) ELISA showing a decrease in IgG3 production of B cells from *Cd23-cre x Nfatc1*$^{flx/flx}$ mice upon culture for 6 d. (D) Decreased IgG$^+$ plasmablast formation of B cells from *Cd23-cre x Nfatc1*$^{flx/flx}$ mice upon 3 d in culture. Flow cytometry of CD19$^+$-gated B cells. In the columns data from three assays are compiled. (E and F) Diminished

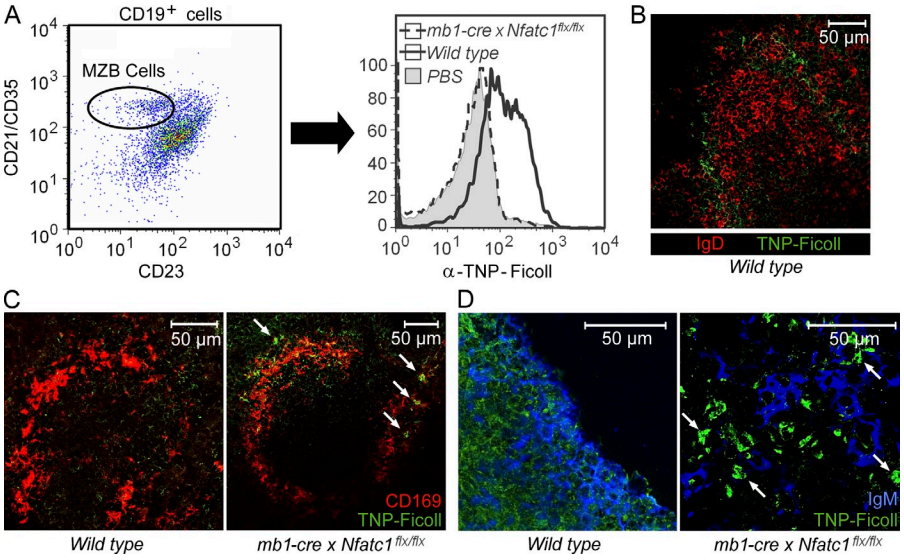

Figure 5. TNP-Ficoll antigen does not bind to NFATc1$^{-/-}$ MZB cells, but forms large aggregates in spleen. 150 µg TNP-Ficoll was injected i.v., and 1 h later splenic B cells were prepared for flow cytometry (A) or spleens were taken for histochemical staining (B–D). In A, binding of antigen to MZB cells was determined by staining with APC-labeled α-TNP-Ficoll. In B–D, histochemical stainings were performed using α-TNP-Ficoll, α-IgD, α-CD169/MOMA-1, and α-IgM. Typical results from three injection experiments are shown.

with WT mice 1, 2, or 3 wk after primary injection. Again, the differences in IgM serum levels were smaller after 2 and 3 wk of immunization, but statistically significant (Fig. 4 A).

These in vivo data are supported by the Ig class switch to IgG3 in cultured B cells. Although in cultures of splenic B cells circular RNA transcripts of IgG3 switch region could be detected in WT B cells after 2 d, no circular transcripts were observed in NFATc1$^{-/-}$ B cells, whereas circular IgG1 transcripts could be detected in both WT and NFATc1$^{-/-}$ B cells (Fig. 4 B). Measuring of secreted IgM and IgG3 antibodies revealed a decrease in IgG3 secretion of ∼50% compared with WT cells (Fig. 4 C). After culturing B cells for 5 d, the percentage of CD138^{+} IgG3^{+} plasmablasts generated from NFATc1$^{-/-}$ cells decreased to ∼30% of IgG3^{+} WT plasmablasts (Fig. 4 D). This might be caused, in part, by a decrease in proliferation and increase in AICD. Indeed, this was found for NFATc1$^{-/-}$ CD138^{+} plasma cells in vitro (Fig. 4, E and F).

The Ig switch to IgG3 by TI-type II antigen takes place in B cells expressing high levels of NFATc1. This was shown by measuring NFATc1, IgM, and IgG3 levels in preparations of splenocytes from *Nfatc1-Egfp* reporter mice upon immunization with NP-Ficoll by flow cytometry. A high level of NFATc1 expression was detected for IgM^{+}IgG3^{+} B cells, whereas B cells expressing only IgM expressed less NFATc1 (Fig. 4 G). NFATc1/GFP^{high} cells also expressed high levels of the GC markers PNA and Fas, the plasma cell marker CD138, and the activation marker CD69 (Fig. 4 G), indicating a close link between NFATc1 expression and Ig class switch.

TI-II antigens rapidly stimulate MZBs to produce IgM and IgG3, and defects in Ig class switch upon TI-II antigen immunization are often correlated with a decrease or lack of MZB cells (Martin and Kearney, 2002; Lopes-Carvalho and Kearney, 2004). Surprisingly, we did not notice a reproducible decrease in population of MZB cells in spleens of mice bearing NFATc1$^{-/-}$ B cells, but defects in their function. When we injected TNP-Ficoll into mice and measured its binding to B cells, we observed a decrease in binding of TNP-Ficoll to NFATc1$^{-/-}$ MZB cells, compared with MZB cells in WT mice. This is shown in Fig. 5 A for 8–9 mo old mice, whereas in younger 7–8-wk-old mice a 40–60% reduction in TNP-Ficoll binding was observed (unpublished data). 1 h after i.v. injection, TNP-Ficoll formed a ring like structure in the marginal zone of B cell follicles, distal of IgD^{high} B2 cells and associated with metallophilic macrophages (Fig. 5, B and C). Whereas in spleen from WT mice TNP-Ficoll was found to be evenly distributed and closely associated with IgM^{high} MZBs, larger aggregates of antigen were detected around, but not associated with CD169^{+} macrophages and IgM^{high} MZB cells in mice with NFATc1$^{-/-}$ B cells (Fig. 5, C and D, white arrows). Similar deposits of antigen aggregates were described upon TNP-Ficoll immunization of mice deficient in Pyk-2, complement C3, or complement receptor CR1/2. All of these mice exhibit marked defects in MZB cells (Guinamard et al., 2000).

Contrary to the immunizations with TI-type II antigen, we did not detect remarkable differences in Ig class switch upon immunization with NP-KLH, a T cell–dependent (TD) antigen. Injections of four WT and four *Cd23-cre x Nfatc1$^{fix/fix}$* mice with NP-KLH (in alum) revealed only subtle, albeit statistically significant differences in serum levels of IgG2a one and two wks of immunization, but no differences in IgM, IgG1 and IgG2b levels (Fig. S5 C). On the same hand, no differences were detected in the affinity of IgG1 serum antibodies generated in WT and *Cd23-cre x Nfatc1$^{fix/fix}$* mice (Fig. S5 D). This shows that in contrast to the strong effect on Ig class

proliferation (E) and increased AICD (F) of CD138^{+} plasmablasts generated from B cells of *Cd23-cre x Nfatc1$^{fix/fix}$* mice upon 3 d culture. (G) Strong *Nfatc1-Egfp* reporter gene expression in plasmablast-like B cells upon immunization of mice with NP-Ficoll. Flow cytometry of splenic B cells showing GFP and IgM+IgG3, PNA^{+}FAS, CD138, or CD69 expression, respectively. In E–G, one typical experiment from three assays is shown. Error bars show ± the SEM.

switch by TI-type II antigens, inactivation of NFATc1 in B cells exerts a mild, if any effect on Ig class switch by TD antigens in the primary response.

NFATc1 affects the regulatory capacity of B cells in vitro and in vivo

B cells control immune reactions by presenting antigens to T cells by releasing cytokines and secreting humoral antibodies. When we tested the effect of NFATc1$^{-/-}$ C57BL/6 B cells on allogenic T cells from BALB/c mice in MLCs we observed a stronger stimulatory activity of WT B cells than NFATc1$^{-/-}$ B cells on T cell proliferation and IL-2 synthesis. This indicates NFATc1$^{-/-}$ B cells as poor activators of T cells (Fig. 6, A and B). This conclusion found support in the weak stimulatory capacity of NFATc1$^{-/-}$ B cells presenting an OVA peptide ($OVA_{323-339}$) to syngenic CD4^{+} T cells from OTII mice that are transgenic (tg) for an OVA-specific TCR (Fig. 6, C and D; Barnden et al., 1998), and NFATc1$^{-/-}$ c2$^{-/-}$ double KO B cells displayed even less stimulatory activity (Fig. S6).

Several lines of evidence indicated that B cells can suppress immune reactions by secreting IL-10, and thereby affect the course of autoimmune diseases (Bouaziz et al., 2008; Lampropoulou et al., 2010). Compared with splenic B cells from WT mice, splenic B cells from *Cd23-cre x Nfatc1$^{flx/flx}$* mice harbor twofold more CD19^{+}CD5^{+}CD1d^{high} B cells that were described to produce IL-10 (Fig. 7 A; Matsushita et al., 2008). Upon treatment by LPS for 24 h (and, in addition, by T+I for the last 8 h) in vitro, the percentage of IL-10–producing CD5^{+}CD1d^{high} B cells increased twofold (Fig. 7 B; note the lack of any IL-10 signal for splenic B cells from IL-10$^{-/-}$ mice). A similar increase in the percentage of IL-10–producing CD138^{+} plasmablasts was detected upon differentiation of NFATc1$^{-/-}$ splenocytes for 3 d in vitro (Fig. 7 C). Incubation with LPS, but not α-IgM, led to a strong increase in IL-10 secretion of both WT and NFATc1$^{-/-}$ B cells, again with higher IL-10 levels for NFATc1$^{-/-}$ than for WT B cells (Fig. 7 D). By adding B cells from WT or *Cd23-cre x NFATc-1$^{flx/flx}$* mice, which were stimulated overnight with α-IgM or LPS or left unstimulated, to allogenic T cells, NFATc1$^{-/-}$

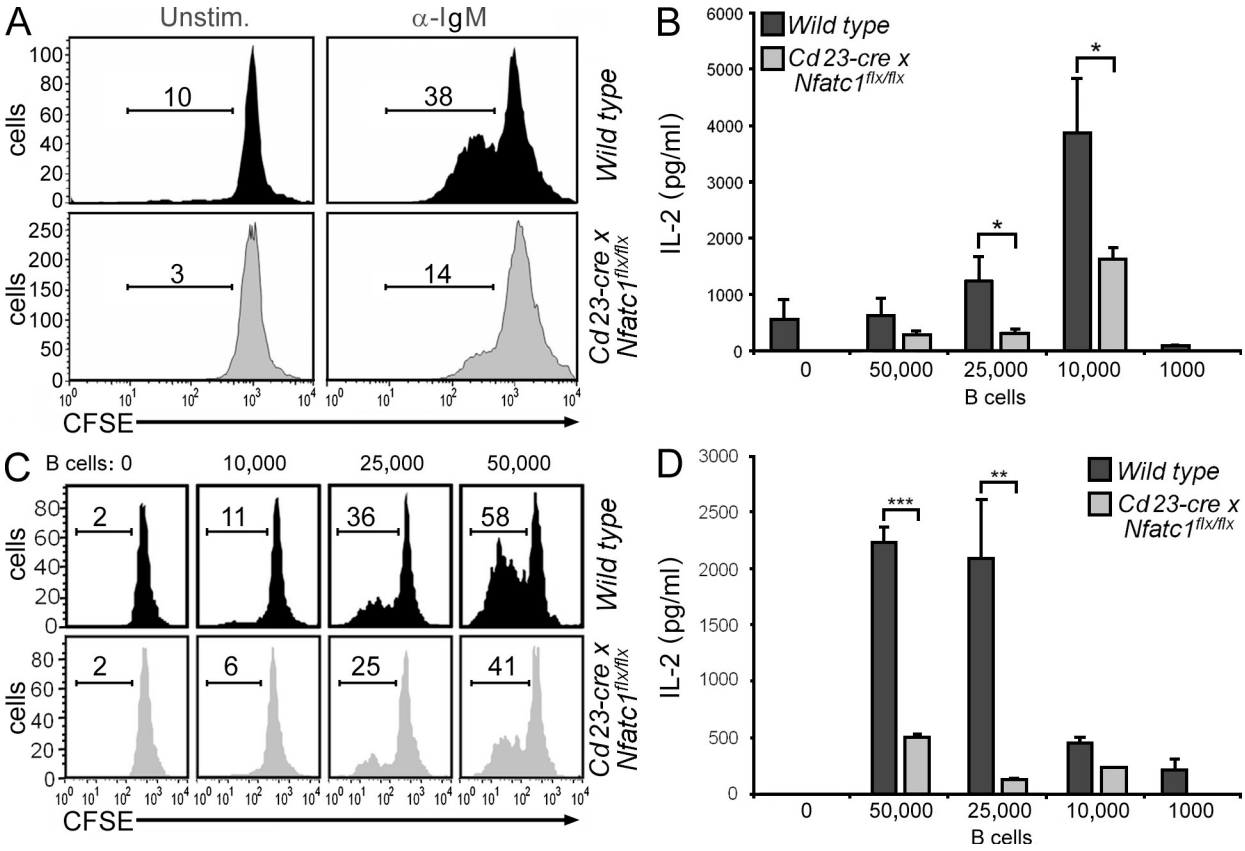

Figure 6. Ablation of NFATc1 in B cells impairs their T cell help. (A and B) MLC. In A, 5 × 10^{4} B cells from C57/BL6 WT or *Cd23-cre x Nfatc1$^{flx/flx}$* mice were incubated with 5 × 10^{4} CFSE-labeled CD4^{+} T cells from a BALB/c WT mouse. After 3 d, proliferation of T cells was measured. In B, B and T cells were cultured as in A and IL-2 secretion was measured by ELISA. In A, one typical assay out of three is shown; in B mean values of two assays are compiled. (C and D) Splenic B cells from WT and *Cd23-cre x Nfatc1$^{flx/flx}$* mice were treated overnight with 10 µg/ml α-IgM and 1 µM (C) or 10 µM $OVA_{323-339}$ peptide (D) followed by incubation with CFSE-stained 5 × 10^{4} T cells from an OTII tg mouse (Barnden et al., 1998) for 3 d. In C, one typical assay out of three is shown. In D, mean values of three experiments are presented.

B cells suppressed the IFN-γ production of T cells, whereas WT B cells did not or only slightly affected T cell IFN-γ expression. This suppressive effect of NFATc1$^{-/-}$ B cells was markedly reduced by adding the IL-10–specific antibody JES5-2A5, which relieved IL-10–mediated inhibition of cytokine production of T cells by B cells (Lampropoulou et al., 2008). A very strong suppressive effect on IFN-γ production was exerted by recombinant IL-10 that could be relieved by adding α-IL-10. By adding α-IL-10 to T cell co-cultures, in part the suppressive effect of NFATc1$^{-/-}$ B cells could be relieved (Fig. 7 E), suggesting that an increase in IL-10 production by NFATc1$^{-/-}$ splenic B cells contributes to suppression of T cell proliferation in vitro.

These in vitro findings prompted us to investigate whether NFATc1$^{-/-}$ B cells affect the clinical course of mouse EAE (Hur et al., 2007), a mouse model for human multiple sclerosis,

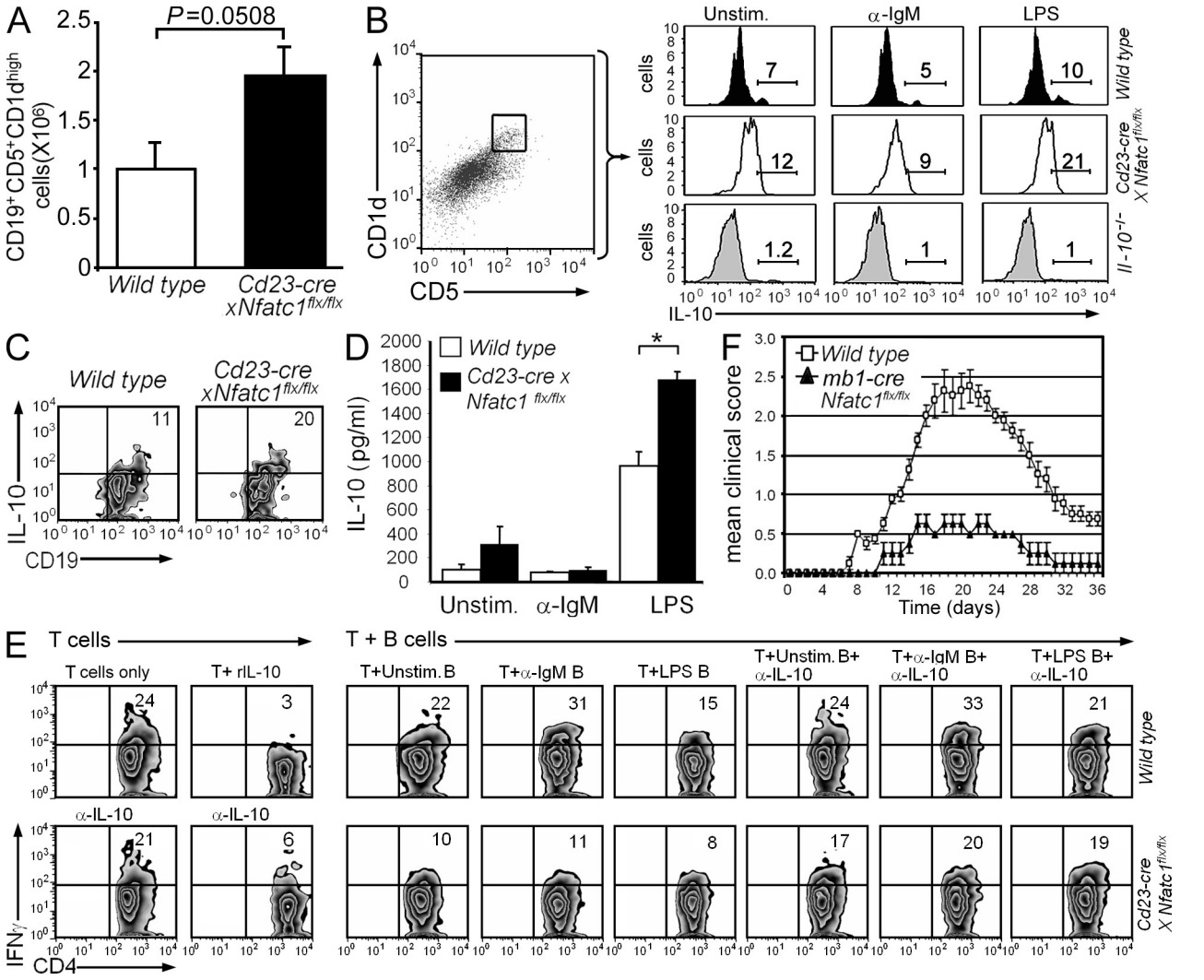

Figure 7. NFATc1 ablation leads to an increase in IL-10 production and amelioration of the clinical course of EAE. (A) Increased CD19^{+}CD5^{+}CD1d^{high} B cell number in spleen freshly prepared from *Cd23-cre X Nfatc$^{flx/flx}$* mice, compared with WT mice. Six individual mice were investigated, and mean values are shown. (B) IL-10 production of unstimulated CD5^{+}CD1d^{high} NFATc1$^{-/-}$ B cells or cells treated with α-IgM or LPS (10 µg/ml each) for 24 h and with T+I for the last 8 h. Cells were stained with antibodies directed against CD1d and CD5, and against IL-10 for intracellular flow cytometry. Shown are the results of one (out of five) typical experiment of IL-10 stains of CD5^{+}CD1d^{high} B cells. (C) Increase in IL-10–producing CD138^{+}CD19^{+} plasmablasts after 3 d in culture with LPS (and T+I for the last 6 h) in preparations of splenocytes from mice bearing *Cd23-cre x Nfatc1$^{flx/flx}$* B cells. One typical assay out of three is shown. (D) IL-10 production by unstimulated WT and NFATc1$^{-/-}$ splenic B cells and cells stimulated by α-IgM or LPS for 72 h in culture. IL-10 was measured in ELISA, and mean values of three assays are shown. (E) MLC. Decreased IFN-γ production by CD4^{+} T cells incubated for 48 h in the presence of 0.5 µg/ml α-CD3 and, during the last 6 h, with T+I, without B cells or with unstimulated B cells or B cells prestimulated by α-IgM or LPS for 24 h from WT or *mb1-cre x Nfatc1$^{flx/flx}$* mice. As indicated, 5 ng/ml recombinant IL-10 and/or 1 µg/ml of IL-10–specific antibody JES5-2A5 (Lampropoulou et al., 2008) were added to the cultures. One typical set out of three assays is shown. (F) EAE. By injection of MOG_{35-55} peptide in complete Freund's adjuvant, and pertussis toxin at day 2 (Pierau et al., 2009), EAE was induced in *mb1-cre x Nfatc1$^{flx/flx}$* and WT mice as indicated. The data show the mean clinical score + SEM from 3 independent experiments, with $n = 9$ (WT) and $n = 14$ (*mb1-cre x Nfatc1$^{flx/flx}$*) mice.

which is strongly affected by IL-10 (Fillatreau et al., 2002; Bouaziz et al., 2008). By inducing adjuvant-driven EAE (Pierau et al., 2009) in *mb1-cre x NFATc1$^{flx/flx}$* and WT mice, we observed that NFATc1 ablation in BM B cells resulted in a much milder EAE than in control mice. Whereas in control mice the onset of EAE was detected 7–8 d after MOG_{35-55} peptide injection reaching EAE scores of 2–2.5 at day 20, for *mb1-cre* x *Nfatc1$^{flx/flx}$* mice first EAE signs were obvious at day 11 upon MOG_{35-55} injection, reaching scores of 0.5–1.0 (Fig. 7 F). This shows that the expression of NFATc1 in B cells enhances the severity of EAE.

DISCUSSION

The results of this study show that ablation of NFATc1 in committed BM pro-B cells or in splenic B cells exerts a relative mild effect on the overall differentiation of peripheral B cells. Peritoneal $CD5^+$ B1a cells are the notable exception because their generation is strictly dependent on NFATc1 expression (Fig. S2, E and F; Berland and Wortis, 2002, 2003). However, although NFATc1 activity seems to play a minor role in the development of B cells in BM and periphery, it is of crucial importance for the fate and function of B cells upon BCR triggering. Our data show that NFATc1 controls (a) the proliferation and AICD of splenic B cells (and plasmablasts) upon BCR stimulation, (b) the Ig class switch to IgG3 by the TI-type II antigen NP-Ficoll and the formation of $IgG3^+$ plasmablasts in vitro, (c) the IL-10 production of $CD1d^{high}CD5^+$ B cells that suppressed the IFN-γ production by and proliferation of co-cultivated $CD4^+$ T cells, and (d) the clinical course of MOG-peptide/adjuvant-driven EAE, a mouse model of human multiple sclerosis. Because NFATc1 ablation led to a marked decrease in the release of Ca^{2+} from endoplasmic stores, Ca^{2+} influx and Cn activity as well as in distinct changes in expression of genes that affect (or are affected by) Ca^{2+} levels, one may conclude that NFATc1 controls Ca^{2+} flux and Cn activity in peripheral B cells.

NFATc1$^{-/-}$ B cells share several characteristics with B cells from mouse models in that individual components of BCR signaling cascade have been inactivated. Such as with mice deficient for Btk (Kerner et al., 1995; Khan et al., 1995), PLC-γ2 (Hashimoto et al., 2000; Wang et al., 2000), and SLP-65/BLNK (Jumaa et al., 1999; Pappu et al., 1999; Xu et al., 2000), and with Igα$^{Y204F/Y204F}$ 'knock in' (k.i.) mice (Patterson et al., 2006). Similar to *mb1-cre x Nfatc1$^{flx/flx}$* mice, these mice have a severe block in the generation of B1a cells and in Ig class switch upon immunization with TI-type II, but not TD antigens, and their B cells are characterized by a marked diminished Ca^{2+} flux and BCR-mediated proliferation. However, contrary to B cell development in *mb1-cre x Nfatc1$^{flx/flx}$* mice, SLP-65$^{-/-}$ mice show a defect at the pre–B cell stage (of $CD43^+BP1^+IgM^-$ cells) in BM and, therefore, a drastic reduction in number of peripheral B cells (Jumaa et al., 1999). Unlike B cells from *mb1-cre x Nfatc1$^{flx/flx}$* and SLP-65$^{-/-}$ mice, Igα$^{Y204F/Y204F}$ k.i. B cells did not show an impaired survival in vitro (Patterson et al., 2006). These observations indicate that NFATc1$^{-/-}$ B cells share several, but not all properties with those mice defective in individual components of BCR signaling. However, collectively, the phenotype of NFATc1$^{-/-}$ B cells indicates that the induction of NFATc1 represents an important molecular event of BCR signaling that transmits antigenic signals from the BCR to NFATc1 and, finally, to the numerous NFATc1 target genes that control the proliferation, AICD, cytokine production and TI-type II antigen–mediated Ig switch of splenic B cells.

The diminished release of Ca^{2+} from intracellular stores and the decrease in Ca^{2+} influx in NFATc1$^{-/-}$ B cells suggest NFATc1 as a key molecule in adjusting the levels of free intracellular Ca^{2+} in B cells. Although it is currently unknown how NFATc1 controls these signaling events, the expression (or activation) of molecules involved in early BCR signaling controlling Ca^{2+} release from endoplasmic stores seem to be under NFATc1 control. One prominent candidate gene is the *Cd22* gene, whose expression is enhanced in NFATc1$^{-/-}$ B cells. Inactivation of the *Cd22* gene, on the other hand, resulted in an increase of NFATc1/αA levels in unstimulated B cells and B cells treated with LPS (Fig. S4 F). CD22 affects BCR signals by recruiting the tyrosine phosphatase SHP-1 upon phosphorylation of its multiple motifs, and it is likely that SHP-1 affects the phosphorylation of members of BCR cascade, such as of Btk, SLP-65, or PLC-γ2 that control Ca^{2+} release through activating IP_3 receptors (Nitschke, 2009).

It is currently unknown whether CD22 is the only (or major) target through which NFATc1 affects Ca^{2+} flux. The expression of human SERCA3 (*ATP2A3*) gene in endothelial cells and mouse IP_3R1 (*Itpr1*) gene in hippocampal neurons have been described to be under NFAT control (Graef et al., 1999; Hadri et al., 2006), but studies on IP_3R1 expression in T cells (Nagaleekar et al., 2008) did not reveal a positive effect of NFATs on IP_3R1 expression in these cells. Likewise, the expression of PLC-γ2, Btk, and SLP-65 appeared to be quite normal in NFATc1$^{-/-}$ B cells (unpublished data). However, large proteins such as IP_3R1 and PLC-γ2 are expressed from very complex genes that, like the *Rcan1* and *Nfatc1* genes, might be under the control of multiple promoters and/or poly A sites and alternately spliced. It remains to be shown whether this is true for other molecules of BCR signaling.

Prominent upstream NFAT targets of Ca^{2+}/Cn cascade are *Rcan1*, the gene encoding the Cn inhibitor calcipression/DSCR1, and the *Ppp3cb* gene expressing CnA β, the β form of catalytic subunit A of Cn in lymphocytes. For both the *Rcan1-4* and *Ppp3cb* promoters, arrays of NFAT motifs have been described, and the binding of NFAT factors to these promoters has been reported for nonlymphoid cells (Rothermel et al., 2003; Oka et al., 2005). Our data indicate that in B cells Rcan1, CnA β, and NFATc1 form a regulatory network (Fig. S5 A) that helps to fine tune the proper expression of NFATc1, in particular of NFATc1/αA, and the activation of further NFATc factors during immune responses.

NFATc1 expression supports BCR-mediated proliferation and suppresses AICD of primary B cells (Fig. 2), e.g., in the early clonal expansion phase of an immune response. Although there are several studies on a direct NFAT-mediated

regulation of cell cycle mediators in T cells (Baksh et al., 2002; Caetano et al., 2002; Carvalho et al., 2007), in our microarray studies among the numerous *cyclin*, *cdk*, or *cell cycle* inhibitor genes we detected only the *Ccnb1* gene, encoding Cyclin B1, as a putative NFATc1 target gene in B cells (Table S1). This finding led us to conclude that in B cells, NFATc1 enhances numerous genes controlling cell cycle at moderate levels, and gene set enrichment analyses (Table I) support this view. One exception might be the *Bcl2* gene (Table S2) that, in addition to its role in apoptosis, was described to retard cell cycle entry (Vairo et al., 2000). However, the detection of proapoptotic factors FasL, PD-1, and Light molecules as direct NFATc1 target and own experimental data (unpublished data) suggest that at very high concentrations NFATc1/αA could also act in a proapoptotic manner, killing the majority of amplified lymphocytes at the end of an immune response. But further experiments using more appropriate mouse models are necessary to substantiate this hypothesis.

The increase in $CD1d^{high}CD5^{+}$ B cells producing IL-10 suggests that NFATc1 affects the regulatory capacity of B cells. The *Il10ra* gene belongs to the 37 genes whose expression was markedly increased in $NFATc1^{-/-}$ B cells (Table S2), and in 2 out of 3 microarray assays a similar increase was detected for the *Il10* gene (unpublished data). This implies that the induction of NFATc1 in B cells suppresses, either directly or indirectly, IL-10 production. This conclusion is supported by the α-IgM–mediated decrease in IL-10 synthesis of $CD1d^{high}CD5^{+}$ B cells upon BCR triggering and NFATc1 induction, and suggests that the increase in IL-10–producing B cells contributes to the clinical course of EAE in *mb1-cre x* $NFATc1^{flx/flx}$ mice. It has previously been shown that B cells play a key role in recovery from EAE by the secretion of IL-10 (Fillatreau et al., 2002). Along with studies on a regulatory role of B cells in the generation of EAE (Yanaba et al., 2008; Pöllinger et al., 2009), our findings lend support to this observation, but also suggest that an impaired antigen-presentation by $NFATc1^{-/-}$ B cells might ameliorate EAE symptoms (Fig. 6, C and D). In addition to IL-10, other candidates that affect EAE are IFN-γ and osteopontin/*Spp1* (Hur et al., 2007), which are both encoded by top ten NFATc1 target genes (Fig. 2 and Table S1).

Collectively, the data of our study show that the induction of NFATc1 plays an important role in the activation and function of splenic B cells upon BCR stimulation. Missing or incomplete NFATc1/αA induction appears to be one reason for the generation of B cell unresponsiveness whereas uncontrolled NFATc1/αA expression could lead to unbalanced immune reactions and autoimmune diseases. Experiments are in progress to elaborate more details of this view.

MATERIALS AND METHODS

Mice, cell isolation and cell cultures. The B cell stage-specific cre lines *mb1 (Cd79a)-cre* (Hobeika et al., 2006), *Cd23-cre*, and *Aicda-cre* (Kwon et al., 2008) have been described previously. Mice bearing a conditional allele of *Nfatc1* (*Nfatc1*^{flx}; also designated as *Nfat2*^{flx}) were generated by K. Mark Ansel, M.R. Müller, and A. Rao (Harvard Medical School, Boston, MA) by flanking exon 3 of the mouse *Nfatc1* gene with loxP sites (to be described in detail elsewhere). All of the following gene-deficient mice were published previously: Btk (Khan et al., 1995); SLP-65 (Jumaa et al., 1999); IL-10 (Kühn et al., 1993); CD22 (Nitschke et al., 1997); Light (Scheu et al., 2002); and PD-1 (Nishimura et al., 1999). Transgenic *Nfatc1-Egfp* reporter mice were created upon insertion of a *Egfp* cDNA into exon 3 of mouse *Nfatc1* locus cloned in a BAC vector spanning ∼210 kb *Nfatc1* DNA. Details of those BAC-tg mice will be published elsewhere. Animal experiments were performed according to project licenses (55.2–2531.01-53/10B), which are approved and controlled by the Regierung von Unterfranken, Würzburg. In most of experiments, 6–8-wk-old mice were used. Naive splenic B cells were isolated using Miltenyi Biotec cell isolation kit to a purity of 95–98% as determined by flow cytometry. 0.5–1 × 10^6 cells were cultured in 200 µl X-vivo 15 medium (Lonza) and stimulated with 10 µg/ml LPS (Sigma-Aldrich), 1–10 µg/ml α-IgM ($F(ab')_2$ fragment goat anti–mouse IgM; Jackson ImmunoResearch Laboratories), 1 or 2 µg/ml α-CD40 (R&D Systems) or TPA and ionomycin as specified in the figure legends. Cell cultures were supplemented with $CaCl_2$ as specified, and/or with the Cn inhibitors cyclosporin A and FK506, or the NFAT inhibitor 11R-Vivit (EMD). Because of its better solubility and cellular penetration, 11R-Vivit was dissolved in DMSO and used in concentrations between 0.1 and 10 µM. Because DMSO itself interfered with B cell survival, the effect of DMSO on B cells was tested in parallel assays.

Naive $CD4^{+}$ T cells were isolated using a $CD4^{+}$ T cell isolation kit (Miltenyi Biotec), stained with CFSE and incubated with B cells that were preactivated overnight by incubation with 10 µg/ml α-IgM. IL-2 secretion of T cells was measured with a Ready-Set-Go ELISA kit (eBioscience).

EAE induction. Mice were immunized with 200 µg of myelin oligodendrocyte ($MOG_{35–55}$) peptide in CFA (Sigma-Aldrich) containing 800 mg of heat-killed *Mycobacterium tuberculosis* (Difco) as described previously in detail (Pierau et al., 2009). Animal experiments were approved by the state authorities of the Land Sachsen-Anhalt. Mice with a clinical score >2.5 were killed according to the animal statutes. The MOG peptide was provided by D. Rheinhold (Institute of Medical and Clinical Immunology, Magdeburg, Germany).

Gene expression analysis and statistical evaluation. B cells from WT and *mb1-cre x* $Nfatc1^{flx/flx}$ mice were left unstimulated or stimulated with 10 µg/ml α-IgM for 3, 8, and 16 h, respectively. Their RNA was isolated from frozen cells using the TRIzol reagent (Invitrogen). Gene expression analysis was performed in three biological replications using the mouse whole genome 430 2.0 gene expression arrays from Affymetrix. The data were normalized to 500 arbitrary units (MAS5) using the Gene Chip Operating Software (GCOS) from Affymetrix. For statistical analysis absent signals were floored to a common baseline (50 U) and expression values were $\log_2$ transformed.

To compare the gene expression profiles between the WT and $Nfatc1^{-/-}$ phenotypes for any given time point (3, 8, and 16 h after α-IgM stimulation), data were time zero transformed and sorted for differential expression. Genes that showed at least a twofold difference in expression in all three replicates were determined by overlap analysis using Access. Gene set enrichment analysis (GSEA; http://www.broad.mit.edu/gsea) was performed as described (Subramanian et al., 2005) using 81 lymphoma associated gene signatures published previously (Shaffer et al., 2001) from the signature database of the Staudt laboratory http://lymphochip.nih.gov/signaturedb/ and 1.687 curated gene sets (c2) from the Molecular Signatures Database (MSigDB; Subramanian et al., 2005). Because both phenotypes that were compared in this approach consisted of less than seven samples, "gene set" was chosen as permutation type in the settings of the GSEA software, as recommended by the GSEA team.

The signatures and gene sets were regarded as significantly enriched when the nominal P value and the tail area FDR (tail area false discovery rate) were less than 0.05 and 0.25, respectively. A selective leading edge analysis was performed using significantly enriched gene sets to extract the genes that account for the enrichment score.

For visualization of the data the Cluster and TreeView software packages provided by M. Eisen (http://rana.lbl.gov/EisenSoftware.htm; University of California, Berkeley, Berkeley, CA) were used.

Western blotting. Western blots were performed by separation of whole protein extracts on PAGE-SDS gels followed by immunodetection of NFATc1 using the 7A6 mAb (obtained from BD or Santa Cruz Biotechnology) or polyclonal antibodies (pAB) specific for NFATc1 or NFATc2 (ImmunoGlobe). For detecting NFATc1/αA (Fig. 1 B), a pAb raised against the NFATc1 α-peptide (ImmunoGlobe) was used. As loading control, filters were stained by Ponceau red. Signals were developed by chemiluminescence detection using Super Signal (Thermo Fisher Scientific).

Apoptosis assays and flow cytometric analysis. Apoptosis assays were performed by staining with propidium iodide (PI, 125 μg/ml) and Annexin V-FITC (BD), incubated for 15 min at 37°C and analyzed on FACSCalibur using CellQuest software (BD) and FlowJo (Tree Star, Inc.). Electronic compensation of the instrument was done to exclude overlapping emission spectra. In total, 10,000 events were acquired, the cells were gated, and dual parameter dot plots of FL1-H (x-axis; FITC-fluorescence) versus FL2-H (y-axis; PI-fluorescence) were gated in logarithmic fluorescence intensity. For IL-10 detection in specific B cell subset, nonstimulated cells or cells stimulated with α-IgM or LPS were treated by T+I and GolgiPlug for the last 8 h, blocked with mouse Fc receptor specific mAb (BD) and stained with CD5 PE and CD1d FITC mouse-specific antibodies (BD). Cells were fixed and permeabilized using the eBioscience fixing and permeabilizing kit according to manufacturer's instructions. Next, cells were stained with anti–mouse IL-10 APC antibody (eBioscience). Unstimulated cells and isotype controls were also used in flow cytometric analysis.

For the determination of cell cycle phase distribution of nuclear DNA, cells were first fixed in 100% methanol, permeabilized, and nuclear DNA was labeled with PI (125 μg/ml) after RNase (10 μl from 2 mg/ml stock) treatment. Cell-cycle phase distribution of nuclear DNA was determined on a FACSCalibur using CellQuest software, fluorescence (FL2-A) detector equipped with a 488-nm Argon laser light source and a 623-nm band pass filter (linear scale). In total, 10,000 events were acquired for analysis. CellQuest and FlowJo statistics was used to quantify the data at different phases of the cell cycle. Histogram display of FL2-A (x axis, PI-fluorescence) versus counts (y axis) has been displayed in Fig. S3 C.

Immunizations and ELISAs. NP-Ficoll (10 μg/mouse in PBS) or NP-KLH (100 μg/mouse, Alum precipitated) was i.p. injected into age-matched mice. Levels of NP-specific antibodies were determined by ELISA with 10 μg/ml NP-BSA coated MaxiSorp plates (Nunc). A sample of pooled sera from days 7 and 21 was used as standard and included on every ELISA plate. Total Ig titers from naive mice were determined by ELISA on PolySorp plates (Nunc) coated with isotype-specific antibodies and monoclonal antibody, and isotype antibodies served as standards (SouthernBiotech). Serum samples were applied as serial dilutions, and their concentration was quantified against the standard curve. Isotype-specific antibodies coupled to alkaline phosphatase were used for detection.

In vitro class-switching assays. 10^6 splenocytes were cultured in 1 ml X-vivo medium without or with LPS (10 μg/ml) or with LPS + IL-4 (10 ng/ml) for 2 d, followed by RNA extraction with TRIzol and cDNA synthesis using the iScript cDNA Synthesis kit (Bio-Rad Laboratories). PCR reactions were performed with the primers for the detection of IgG3 and IgG1 circular transcript as described (Kinoshita et al., 2001). 2.5×10^5 splenocytes were cultured in 1 ml X-vivo medium and stimulated without or with LPS for 6 d. Supernatants were collected and subjected to ELISA. Unlabeled goat anti–mouse IgM and IgG3 were used to coat ELISA plates, mouse IgM and IgG3 (0.1 mg/ml each) were used as standards, and alkaline phosphatase–coupled, isotype-specific antibodies were used for detection. Splenocytes stimulated with LPS for 3 d were stained with antibodies directed against CD19, CD138, and IgG1 and/or IgG3 for the detection of Ig class switch.

In vitro IL-10 secretion assay. 4×10^4 cells were incubated in 200 μl X-vivo medium with or without α-IgM or LPS for 72 h, and supernatants were collected. ELISA was performed using a mouse IL-10 ELISA kit (eBioscience) according to the manufacturer's instructions.

Immunohistochemistry. For antigen localization (Fig. 5), 150 μg TNP-Ficoll was injected into the tail vein of mice. 60 min later, B cells were prepared for flow cytometry from one part of the spleen, and the other part was used for histological examination. Cryosections were stained with biotin-conjugated hamster α-TNP-Ficoll IgG (BD), α-CD169/MOMA-1 (Serotec), α-IgD, or α-IgM (SouthernBiotech).

For nuclear localization of NFATc2 (Fig. 3 F), splenic B cells stimulated for 24 h by 10 μg/ml α-IgM and 5 μg/ml α-CD40 and stimulated by T+I for 30 min were harvested by cytospin, dried overnight, fixed in acetone, and stained with antibodies directed against NFATc2 (BD or Santa Cruz Biotechnology). Nuclear localization of NFATc2 in 100 cells from three individual experiments was determined by confocal microscopy.

Calcium measurements. 5×10^6 of freshly prepared murine splenic B cells were incubated in 700 μl X-vivo medium or RPMI 1640 (Invitrogen) containing 5% FCS (PAN), 1 μM Indo-1-AM (Invitrogen), and 0.015% Pluronic F127 (Invitrogen) at 30°C for 25 min. The cell suspension was then diluted with 700 μl medium containing 10% FCS and incubated at 37°C for another 10 min. The cells were washed twice with Krebs-Ringer solution containing 10 mM Hepes, pH 7.0, 140 mM NaCl, 4 mM KCl, 1 mM $MgCl_2$, 1 mM $CaCl_2$, 10 mM glucose, and 0.5 mM EGTA and diluted to a concentration of 10^7 cells per ml. For measurement, the cells were diluted 1:10 in Krebs-Ringer solution and a baseline was recorded for 60 s. Ca^{2+} movement was assessed after stimulation of the cells with α-IgM (Jackson ImmunoResearch Laboratories), followed by the addition of Ca^{2+} in denoted concentrations after 2 min of recording. Increases in free intracellular Ca^{2+} were measured in real-time on a LSR II (BD). Raw data files were transferred to FlowJo software and are presented as a median and in comparative overlay analyses.

Determination of Cn activity and cellular CnA levels. Cn activity of freshly prepared naive splenic B cells was determined using BIOMOL's non-radioactive Cn kit according to the manufacturer's instructions. In brief, 3×10^7 splenic B cells were lysed in 50 μl of lysis buffer (+ protease inhibitors) by pipetting and vortexing, followed by high speed centrifugation for 45 min at 4°C in an Eppendorf centrifuge. For removing free phosphate, supernatants were passed through a desalting spin column, stored on ice, or quick-frozen in liquid nitrogen before storage at −70°C. Aliquots of supernatant corresponding to $\sim 3 \times 10^6$ of B cells were tested in 50-μl assays, containing the RII phosphopeptide Cn substrate. The release of free phosphate was determined in a Malachite green assay. Incubations of parallel assays containing either no substrate, or 10 mM EGTA and EGTA+okadaic acid indicated the specificity of Cn reaction. In immunoblots, a CnA α/β-specific antibody (BD) was used to determine CnA levels (Fig. 3 E).

ChIP assays. ChIP assays were performed according to a previously published protocol (Soutoglou and Talianidis, 2002) and slightly modified. In brief, the chromatin of $0.5–1 \times 10^8$ splenocytes was cross-linked using 1% formaldehyde, and the reaction was quenched with 125 mM glycine. Nuclei were isolated and treated with DNase I, sonicated, and, after preclearing with protein A–Sepharose that was blocked with salmon sperm DNA, protein–DNA complexes were immunoprecipitated using an NFATc1 mAb (BD), or an unrelated GST antibody as control. After washing, elution, and reversion of cross-links, DNA was isolated by phenol/chloroform and used in PCR reactions that were performed with the following primers amplifying the promoters of the following genes: *Il2*, forward 5′-CCTGTGTGCAATTAGCTCA-3′ and reverse 5′-CTCTTCTGATGACTCTCTGGA-3′; *Fasl*, forward 5′-ACTTGCTGAGTTGGACCTCA-3′ and reverse 5′-GTAATTCATGGGCTGCTGCA-3′; *Pdcd1*, forward 5′-CAGGCACAGAACGTTCAGGAA-3′ and reverse 5′-AACAGGAGTTAGGGATCACA-3′; *Rcan1*, forward 5′-GCGGCATAGTTCCCACTGGTA-3′ and reverse 5′-GAGTGCTGGGCTTTTCATCCA-3′; *Spp1*, forward 5′-CACACTCTCCATGCCAGAGCA-3′ and reverse 5′-CACAGAGGCCTCTGCTTGTCA-3′; *Tnfsf14*, forward 5′-TGTCCGTCTGTCCATCCACCA-3′ and reverse 5′-GGTGCAAGATGCTTGCATGGA-3′; *Ppp3ca*, forward 5′-TTTTCTTCAGGGTGCCAGTC-3′ and reverse 5′-CAGTCTGTTCCCATCCACCT-3′;

Ppp3cb, forward 5′-GCTTAGACTTTTCCAGCTGA-3′ and reverse 5′-GAGGCTACTACAGAAACGGAA-3′.

RT-PCR assays. RNA was purified using TRIzol reagent (Invitrogen) and first strand synthesis was performed with 1 µg of RNA according to manufacturer's protocol (Fermentas). For PCR reactions, the following primers were used: *Cd22*, forward 5′-TCCCAGACTTTCCCCTCCCTA-3′ and reverse 5′-CAACCACTTTTACCCACTGA-3′; *Nfatc2*, forward 5′-GGGTTCG-GTGAGTGACAGTT-3′ and reverse 5′-CTCCTTGGCTGTTTGGG-ATA-3′; *Nfatc3*, forward 5′-CACGCCGATGACTACTGCAAACTG-3′ and reverse 5′-CCTTGGAGCTGAAATGATGGTGAC-3′.

Statistical analysis. All statistical analysis was performed using SPSS software. The Mann–Whitney test was used to evaluate the significance of differences in Cn measurements, for other results the unpaired Student's *t* test was used. Differences with P values of 0.05 and less are considered as significant. *, $P < 0.05$; **, $P < 0.005$, and ***, $P < 0.001$. If not stated otherwise, mean values from three assays are shown, or one representative experiment is shown from three similar assays.

Accession nos. The GEO accession no. for microarray data is GSE21063.

Online supplemental material. Fig. S1 shows immunoblots indicating the induction of NFATc1 upon α-CD40 and T+I stimulation and the loss of NFATc1 induction in splenic B cells from *mb1-cre* and *Cd23-cre x Nfatc1$^{flx/flx}$* mice. Fig. S2 shows flow cytometric data on the role of NFATc1 on B cell development in BM, LN, spleen, and peritoneum. Fig. S3 demonstrates the effect of NFATc1 ablation on the proliferation and survival of splenic B cells. In Fig. S4, data are compiled on the effect of novel Cn inhibitor NCI3 on proliferation of splenic B cells, of the NFAT inhibitor VIVIT on proliferation and apoptosis of splenic B cells, of NFATc1 ablation on Ca^{2+} flux, and on CD22 ablation on NFATc1 induction in splenic B cells. Fig. S5 shows a model on the control of Cn-NFAT network by NFATc1; serum Ig levels of nonimmunized WT, *mb1-cre*, *Cd23-cre*, and *Aicda-cre x Nfatc1$^{flx/flx}$* mice; serum Ig levels of WT and *Cd23-cre x Nfatc1$^{flx/flx}$* mice upon immunization with NP-KLH; and the affinity of IgG1 antibody generated upon immunization with anti-NP_4 or anti-NP_{16} KLH. Fig. S6 shows the effect of NFATc1 and NFATc2 ablation on the capacity of B cells to stimulate T cells to produce IL-2 and to proliferate. In Table S1, genes are compiled that were twofold stronger expressed in WT than NFATc1$^{-/-}$ splenic B cells. In Table S2, genes are compiled that were twofold stronger expressed in NFATc1$^{-/-}$ splenic B cells. In Table S3, a leading edge analysis of pathways/gene sets is shown that were significantly enriched in splenic B cells from WT mice compared with those from *mb1-cre x Nfatc1$^{flx/flx}$* mice after 16 h stimulation with α-IgM. Online supplemental material is available at http://www.jem.org/cgi/content/full/jem.20100945/DC1.

We are very much indebted to A. Dietzel, D. Michel, and I. Pietrowski for excellent technical support. We thank Drs. K. M. Ansel (UCSF) and A. Rao (Harvard Medical School) for generating and providing the *Nfatc1$^{flx/flx}$* mice (funded by National Institutes of Health grants CA42471 and AI40127 to A. Rao). For the kind gift of mouse lines we thank Drs. M. Busslinger (Vienna), G. and P. Matthias (Basel), M. Reth (Freiburg), S. Scheu (Düsseldorf), A. Waisman (Mainz) and H. Wiendl (Würzburg). For reagents and advice we are indebted to Drs. R. Baumgrass and M. Sieber (Berlin), N. Beyersdorf (Würzburg), T. Bopp, and E. Schmitt (Mainz), S. Fillatreau (Berlin), M. Lutz (Würzburg), D. Olive (Marseille), D. Reinhold (Magdeburg), and J. Wienands (Göttingen).

The work was supported by the Deutsche Forschungsgemeinschaft grant TRR52 (to F. Berberich-Siebelt, A. Avots, and E. Serfling), SFB643 and FOR832 Erlangen (to L. Nitschke), and BO 1054-2/2 (to U. Bommhardt); the Land Sachsen-Anhalt (N2/C2 to U. Bommhardt); and the Wilhelm-Sander and Scheel foundations (to E. Serfling).

The authors have not commercial affiliations and declare no competing financial interests.

Submitted: 12 May 2010
Accepted: 8 March 2011

REFERENCES

Aramburu, J., M.B. Yaffe, C. López-Rodríguez, L.C. Cantley, P.G. Hogan, and A. Rao. 1999. Affinity-driven peptide selection of an NFAT inhibitor more selective than cyclosporin A. *Science*. 285:2129–2133. doi:10.1126/science.285.5436.2129

Avots, A., M. Buttmann, S. Chuvpilo, C. Escher, U. Smola, A.J. Bannister, U.R. Rapp, T. Kouzarides, and E. Serfling. 1999. CBP/p300 integrates Raf/Rac-signaling pathways in the transcriptional induction of NF-ATc during T cell activation. *Immunity*. 10:515–524. doi:10.1016/S1074-7613(00)80051-5

Baksh, S., H.R. Widlund, A.A. Frazer-Abel, J. Du, S. Fosmire, D.E. Fisher, J.A. DeCaprio, J.F. Modiano, and S.J. Burakoff. 2002. NFATc2-mediated repression of cyclin-dependent kinase 4 expression. *Mol. Cell*. 10:1071–1081. doi:10.1016/S1097-2765(02)00701-3

Barnden, M.J., J. Allison, W.R. Heath, and F.R. Carbone. 1998. Defective TCR expression in transgenic mice constructed using cDNA-based alpha- and beta-chain genes under the control of heterologous regulatory elements. *Immunol. Cell Biol*. 76:34–40. doi:10.1046/j.1440-1711.1998.00709.x

Berland, R., and H.H. Wortis. 2002. Origins and functions of B-1 cells with notes on the role of CD5. *Annu. Rev. Immunol*. 20:253–300. doi:10.1146/annurev.immunol.20.100301.064833

Berland, R., and H.H. Wortis. 2003. Normal B-1a cell development requires B cell-intrinsic NFATc1 activity. *Proc. Natl. Acad. Sci. USA*. 100:13459–13464. doi:10.1073/pnas.2233620100

Bouaziz, J.D., K. Yanaba, and T.F. Tedder. 2008. Regulatory B cells as inhibitors of immune responses and inflammation. *Immunol. Rev.* 224:201–214. doi:10.1111/j.1600-065X.2008.00661.x

Brentani, H., O.L. Caballero, A.A. Camargo, A.M. da Silva, W.A. da Silva Jr., E. Dias Neto, M. Grivet, A. Gruber, P.E. Guimaraes, W. Hide, et al.; Human Cancer Genome Project/Cancer Genome Anatomy Project Annotation Consortium; Human Cancer Genome Project Sequencing Consortium. 2003. The generation and utilization of a cancer-oriented representation of the human transcriptome by using expressed sequence tags. *Proc. Natl. Acad. Sci. USA*. 100:13418–13423.

Caetano, M.S., A. Vieira-de-Abreu, L.K. Teixeira, M.B. Werneck, M.A. Barcinski, and J.P. Viola. 2002. NFATC2 transcription factor regulates cell cycle progression during lymphocyte activation: evidence of its involvement in the control of cyclin gene expression. *FASEB J.* 16:1940–1942.

Carvalho, L.D., L.K. Teixeira, N. Carrossini, A.T. Caldeira, K.M. Ansel, A. Rao, and J.P. Viola. 2007. The NFAT1 transcription factor is a repressor of cyclin A2 gene expression. *Cell Cycle*. 6:1789–1795. doi:10.4161/cc.6.14.4473

Cho, R.J., M. Huang, M.J. Campbell, H. Dong, L. Steinmetz, L. Sapinoso, G. Hampton, S.J. Elledge, R.W. Davis, and D.J. Lockhart. 2001. Transcriptional regulation and function during the human cell cycle. *Nat. Genet*. 27:48–54.

Chuvpilo, S., M. Zimmer, A. Kerstan, J. Glöckner, A. Avots, C. Escher, C. Fischer, I. Inashkina, E. Jankevics, F. Berberich-Siebelt, et al. 1999. Alternative polyadenylation events contribute to the induction of NF-ATc in effector T cells. *Immunity*. 10:261–269. doi:10.1016/S1074-7613(00)80026-6

Chuvpilo, S., E. Jankevics, D. Tyrsin, A. Akimzhanov, D. Moroz, M.K. Jha, J. Schulze-Luehrmann, B. Santner-Nanan, E. Feoktistova, T. König, et al. 2002. Autoregulation of NFATc1/A expression facilitates effector T cells to escape from rapid apoptosis. *Immunity*. 16:881–895. doi:10.1016/S1074-7613(02)00329-1

Fiering, S., J.P. Northrop, G.P. Nolan, P.S. Mattila, G.R. Crabtree, and L.A. Herzenberg. 1990. Single cell assay of a transcription factor reveals a threshold in transcription activated by signals emanating from the T-cell antigen receptor. *Genes Dev.* 4:1823–1834. doi:10.1101/gad.4.10.1823

Fillatreau, S., C.H. Sweenie, M.J. McGeachy, D. Gray, and S.M. Anderton. 2002. B cells regulate autoimmunity by provision of IL-10. *Nat. Immunol*. 3:944–950. doi:10.1038/ni833

Graef, I.A., P.G. Mermelstein, K. Stankunas, J.R. Neilson, K. Deisseroth, R.W. Tsien, and G.R. Crabtree. 1999. L-type calcium channels and GSK-3 regulate the activity of NF-ATc4 in hippocampal neurons. *Nature*. 401:703–708. doi:10.1038/44378

Guinamard, R., M. Okigaki, J. Schlessinger, and J.V. Ravetch. 2000. Absence of marginal zone B cells in Pyk-2-deficient mice defines their role in the humoral response. *Nat. Immunol*. 1:31–36.

Hadri, L., C. Pavoine, L. Lipskaia, S. Yacoubi, and A.M. Lompré. 2006. Transcription of the sarcoplasmic/endoplasmic reticulum Ca2+-ATPase type 3 gene, ATP2A3, is regulated by the calcineurin/NFAT pathway in endothelial cells. *Biochem. J.* 394:27–33. doi:10.1042/BJ20051387

Hardy, R.R., and K. Hayakawa. 2001. B cell development pathways. *Annu. Rev. Immunol.* 19:595–621. doi:10.1146/annurev.immunol.19.1.595

Hashimoto, A., K. Takeda, M. Inaba, M. Sekimata, T. Kaisho, S. Ikehara, Y. Homma, S. Akira, and T. Kurosaki. 2000. Cutting edge: essential role of phospholipase C-gamma 2 in B cell development and function. *J. Immunol.* 165:1738–1742.

Hobeika, E., S. Thiemann, B. Storch, H. Jumaa, P.J. Nielsen, R. Pelanda, and M. Reth. 2006. Testing gene function early in the B cell lineage in mb1-cre mice. *Proc. Natl. Acad. Sci. USA.* 103:13789–13794. doi:10.1073/pnas.0605944103

Hogan, P.G., L. Chen, J. Nardone, and A. Rao. 2003. Transcriptional regulation by calcium, calcineurin, and NFAT. *Genes Dev.* 17:2205–2232. doi:10.1101/gad.1102703

Hogan, P.G., R.S. Lewis, and A. Rao. 2010. Molecular basis of calcium signaling in lymphocytes: STIM and ORAI. *Annu. Rev. Immunol.* 28:491–533. doi:10.1146/annurev.immunol.021908.132550

Hur, E.M., S. Youssef, M.E. Haws, S.Y. Zhang, R.A. Sobel, and L. Steinman. 2007. Osteopontin-induced relapse and progression of autoimmune brain disease through enhanced survival of activated T cells. *Nat. Immunol.* 8:74–83. doi:10.1038/ni1415

Jumaa, H., B. Wollscheid, M. Mitterer, J. Wienands, M. Reth, and P.J. Nielsen. 1999. Abnormal development and function of B lymphocytes in mice deficient for the signaling adaptor protein SLP-65. *Immunity.* 11:547–554. doi:10.1016/S1074-7613(00)80130-2

Keir, M.E., M.J. Butte, G.J. Freeman, and A.H. Sharpe. 2008. PD-1 and its ligands in tolerance and immunity. *Annu. Rev. Immunol.* 26:677–704. doi:10.1146/annurev.immunol.26.021607.090331

Kenny, P.A., T. Enver, and A. Ashworth. 2005. Receptor and secreted targets of Wnt-1/beta-catenin signalling in mouse mammary epithelial cells. *BMC Cancer.* 5:3.

Kerner, J.D., M.W. Appleby, R.N. Mohr, S. Chien, D.J. Rawlings, C.R. Maliszewski, O.N. Witte, and R.M. Perlmutter. 1995. Impaired expansion of mouse B cell progenitors lacking Btk. *Immunity.* 3:301–312. doi:10.1016/1074-7613(95)90115-9

Khan, W.N., F.W. Alt, R.M. Gerstein, B.A. Malynn, I. Larsson, G. Rathbun, L. Davidson, S. Müller, A.B. Kantor, L.A. Herzenberg, et al. 1995. Defective B cell development and function in Btk-deficient mice. *Immunity.* 3:283–299. doi:10.1016/1074-7613(95)90114-0

King, L.B., and B.D. Freedman. 2009. B-lymphocyte calcium influx. *Immunol. Rev.* 231:265–277. doi:10.1111/j.1600-065X.2009.00822.x

Kinoshita, K., M. Harigai, S. Fagarasan, M. Muramatsu, and T. Honjo. 2001. A hallmark of active class switch recombination: transcripts directed by I promoters on looped-out circular DNAs. *Proc. Natl. Acad. Sci. USA.* 98:12620–12623. doi:10.1073/pnas.221454398

Kolb, J.P., D. Renard, B. Dugas, E. Genot, E. Petit-Koskas, M. Sarfati, G. Delespesse, and J. Poggioli. 1990. Monoclonal anti-CD23 antibodies induce a rise in [Ca2+]i and polyphosphoinositide hydrolysis in human activated B cells. Involvement of a Gp protein. *J. Immunol.* 145:429–437.

Krammer, P.H., R. Arnold, and I.N. Lavrik. 2007. Life and death in peripheral T cells. *Nat. Rev. Immunol.* 7:532–542. doi:10.1038/nri2115

Kraus, M., M.B. Alimzhanov, N. Rajewsky, and K. Rajewsky. 2004. Survival of resting mature B lymphocytes depends on BCR signaling via the Igalpha/beta heterodimer. *Cell.* 117:787–800. doi:10.1016/j.cell.2004.05.014

Kühn, R., J. Löhler, D. Rennick, K. Rajewsky, and W. Müller. 1993. Interleukin-10-deficient mice develop chronic enterocolitis. *Cell.* 75:263–274. doi:10.1016/0092-8674(93)80068-P

Kwon, K., C. Hutter, Q. Sun, I. Bilic, C. Cobaleda, S. Malin, and M. Busslinger. 2008. Instructive role of the transcription factor E2A in early B lymphopoiesis and germinal center B cell development. *Immunity.* 28:751–762. doi:10.1016/j.immuni.2008.04.014

Lajaunias, F., L. Nitschke, T. Moll, E. Martinez-Soria, I. Semac, Y. Chicheportiche, R.M. Parkhouse, and S. Izui. 2002. Differentially regulated expression and function of CD22 in activated B-1 and B-2 lymphocytes. *J. Immunol.* 168:6078–6083.

Lam, K.P., R. Kühn, and K. Rajewsky. 1997. In vivo ablation of surface immunoglobulin on mature B cells by inducible gene targeting results in rapid cell death. *Cell.* 90:1073–1083. doi:10.1016/S0092-8674(00)80373-6

Lampropoulou, V., K. Hoehlig, T. Roch, P. Neves, E. Calderón Gómez, C.H. Sweenie, Y. Hao, A.A. Freitas, U. Steinhoff, S.M. Anderton, and S. Fillatreau. 2008. TLR-activated B cells suppress T cell-mediated autoimmunity. *J. Immunol.* 180:4763–4773.

Lampropoulou, V., E. Calderon-Gomez, T. Roch, P. Neves, P. Shen, U. Stervbo, P. Boudinot, S.M. Anderton, and S. Fillatreau. 2010. Suppressive functions of activated B cells in autoimmune diseases reveal the dual roles of Toll-like receptors in immunity. *Immunol. Rev.* 233:146–161. doi:10.1111/j.0105-2896.2009.00855.x

Liu, D., D.M. Umbach, S.D. Peddada, L. Li, P.W. Crockett, and C.R. Weinberg. 2004. A random-periods model for expression of cell-cycle genes. *Proc. Natl. Acad. Sci. USA.* 101:7240–7245.

Lopes-Carvalho, T., and J.F. Kearney. 2004. Development and selection of marginal zone B cells. *Immunol. Rev.* 197:192–205. doi:10.1111/j.0105-2896.2004.0112.x

Macian, F. 2005. NFAT proteins: key regulators of T-cell development and function. *Nat. Rev. Immunol.* 5:472–484. doi:10.1038/nri1632

Martin, F., and J.F. Kearney. 2002. Marginal-zone B cells. *Nat. Rev. Immunol.* 2:323–335. doi:10.1038/nri799

Matsushita, T., K. Yanaba, J.D. Bouaziz, M. Fujimoto, and T.F. Tedder. 2008. Regulatory B cells inhibit EAE initiation in mice while other B cells promote disease progression. *J. Clin. Invest.* 118:3420–3430.

Matsuura, I., C.Y. Lai, and K.N. Chiang. 2010. Functional interaction between Smad3 and S100A4 (metastatin-1) for TGF-beta-mediated cancer cell invasiveness. *Biochem. J.* 426:327–335. doi:10.1042/BJ20090990

Nagaleekar, V.K., S.A. Diehl, I. Juncadella, C. Charland, N. Muthusamy, S. Eaton, L. Haynes, L.A. Garrett-Sinha, J. Anguita, and M. Rincón. 2008. IP3 receptor-mediated Ca2+ release in naive CD4 T cells dictates their cytokine program. *J. Immunol.* 181:8315–8322.

Nayak, A., J. Glöckner-Pagel, M. Vaeth, J.E. Schumann, M. Buttmann, T. Bopp, E. Schmitt, E. Serfling, and F. Berberich-Siebelt. 2009. Sumoylation of the transcription factor NFATc1 leads to its subnuclear relocalization and interleukin-2 repression by histone deacetylase. *J. Biol. Chem.* 284:10935–10946. doi:10.1074/jbc.M900465200

Nishimura, H., N. Minato, T. Nakano, and T. Honjo. 1998. Immunological studies on PD-1 deficient mice: implication of PD-1 as a negative regulator for B cell responses. *Int. Immunol.* 10:1563–1572. doi:10.1093/intimm/10.10.1563

Nishimura, H., M. Nose, H. Hiai, N. Minato, and T. Honjo. 1999. Development of lupus-like autoimmune diseases by disruption of the PD-1 gene encoding an ITIM motif-carrying immunoreceptor. *Immunity.* 11:141–151. doi:10.1016/S1074-7613(00)80089-8

Nitschke, L. 2009. CD22 and Siglec-G: B-cell inhibitory receptors with distinct functions. *Immunol. Rev.* 230:128–143. doi:10.1111/j.1600-065X.2009.00801.x

Nitschke, L., R. Carsetti, B. Ocker, G. Köhler, and M.C. Lamers. 1997. CD22 is a negative regulator of B-cell receptor signalling. *Curr. Biol.* 7:133–143. doi:10.1016/S0960-9822(06)00057-1

Nurieva, R.I., S. Chuvpilo, E.D. Wieder, K.B. Elkon, R. Locksley, E. Serfling, and C. Dong. 2007. A costimulation-initiated signaling pathway regulates NFATc1 transcription in T lymphocytes. *J. Immunol.* 179:1096–1103.

Oka, T., Y.S. Dai, and J.D. Molkentin. 2005. Regulation of calcineurin through transcriptional induction of the calcineurin A beta promoter in vitro and in vivo. *Mol. Cell. Biol.* 25:6649–6659. doi:10.1128/MCB.25.15.6649-6659.2005

Pappu, R., A.M. Cheng, B. Li, Q. Gong, C. Chiu, N. Griffin, M. White, B.P. Sleckman, and A.C. Chan. 1999. Requirement for B cell linker protein (BLNK) in B cell development. *Science.* 286:1949–1954. doi:10.1126/science.286.5446.1949

Patterson, H.C., M. Kraus, Y.M. Kim, H. Ploegh, and K. Rajewsky. 2006. The B cell receptor promotes B cell activation and proliferation through a non-ITAM tyrosine in the Igalpha cytoplasmic domain. *Immunity.* 25:55–65. doi:10.1016/j.immuni.2006.04.014

Pierau, M., S. Engelmann, D. Reinhold, T. Lapp, B. Schraven, and U.H. Bommhardt. 2009. Protein kinase B/Akt signals impair Th17 differentiation and support natural regulatory T cell function and induced

regulatory T cell formation. *J. Immunol.* 183:6124–6134. doi:10.4049/jimmunol.0900246

Pöllinger, B., G. Krishnamoorthy, K. Berer, H. Lassmann, M.R. Bösl, R. Dunn, H.S. Domingues, A. Holz, F.C. Kurschus, and H. Wekerle. 2009. Spontaneous relapsing-remitting EAE in the SJL/J mouse: MOG-reactive transgenic T cells recruit endogenous MOG-specific B cells. *J. Exp. Med.* 206:1303–1316. doi:10.1084/jem.20090299

Rosenwald, A., G. Wright, W.C. Chan, J.M. Connors, E. Campo, R.I. Fisher, R.D. Gascoyne, H.K. Muller-Hermelink, E.B. Smeland, J.M. Giltnane, et al.; Lymphoma/Leukemia Molecular Profiling Project. 2002. The use of molecular profiling to predict survival after chemotherapy for diffuse large-B-cell lymphoma. *N. Engl. J. Med.* 346:1937–1947.

Rothermel, B.A., R.B. Vega, and R.S. Williams. 2003. The role of modulatory calcineurin-interacting proteins in calcineurin signaling. *Trends Cardiovasc. Med.* 13:15–21. doi:10.1016/S1050-1738(02)00188-3

Scheu, S., J. Alferink, T. Pötzel, W. Barchet, U. Kalinke, and K. Pfeffer. 2002. Targeted disruption of LIGHT causes defects in costimulatory T cell activation and reveals cooperation with lymphotoxin beta in mesenteric lymph node genesis. *J. Exp. Med.* 195:1613–1624. doi:10.1084/jem.20020215

Serfling, E., F. Berberich-Siebelt, S. Chuvpilo, E. Jankevics, S. Klein-Hessling, T. Twardzik, and A. Avots. 2000. The role of NF-AT transcription factors in T cell activation and differentiation. *Biochim. Biophys. Acta.* 1498:1–18. doi:10.1016/S0167-4889(00)00082-3

Serfling, E., S. Chuvpilo, J. Liu, T. Höfer, and A. Palmetshofer. 2006. NFATc1 autoregulation: a crucial step for cell-fate determination. *Trends Immunol.* 27:461–469. doi:10.1016/j.it.2006.08.005

Shaffer, A.L., K.I. Lin, T.C. Kuo, X. Yu, E.M. Hurt, A. Rosenwald, J.M. Giltnane, L. Yang, H. Zhao, K. Calame, and L.M. Staudt. 2002. Blimp-1 orchestrates plasma cell differentiation by extinguishing the mature B cell gene expression program. *Immunity.* 17:51–62.

Shaffer, A.L., A. Rosenwald, E.M. Hurt, J.M. Giltnane, L.T. Lam, O.K. Pickeral, and L.M. Staudt. 2001. Signatures of the immune response. *Immunity.* 15:375–385. doi:10.1016/S1074-7613(01)00194-7

Sieber, M., M. Karanik, C. Brandt, C. Blex, M. Podtschaske, F. Erdmann, R. Rost, E. Serfling, J. Liebscher, M. Pätzel, et al. 2007. Inhibition of calcineurin-NFAT signaling by the pyrazolopyrimidine compound NCI3. *Eur. J. Immunol.* 37:2617–2626. doi:10.1002/eji.200737087

Soutoglou, E., and I. Talianidis. 2002. Coordination of PIC assembly and chromatin remodeling during differentiation-induced gene activation. *Science.* 295:1901–1904. doi:10.1126/science.1068356

Srinivasan, L., Y. Sasaki, D.P. Calado, B. Zhang, J.H. Paik, R.A. DePinho, J.L. Kutok, J.F. Kearney, K.L. Otipoby, and K. Rajewsky. 2009. PI3 kinase signals BCR-dependent mature B cell survival. *Cell.* 139:573–586. doi:10.1016/j.cell.2009.08.041

Strasser, A., and M. Pellegrini. 2004. T-lymphocyte death during shutdown of an immune response. *Trends Immunol.* 25:610–615. doi:10.1016/j.it.2004.08.012

Su, A.I., T. Wiltshire, S. Batalov, H. Lapp, K.A. Ching, D. Block, J. Zhang, R. Soden, M. Hayakawa, G. Kreiman, et al. 2004. A gene atlas of the mouse and human protein-encoding transcriptomes. *Proc. Natl. Acad. Sci. USA* 101:6062–6067.

Subramanian, A., P. Tamayo, V.K. Mootha, S. Mukherjee, B.L. Ebert, M.A. Gillette, A. Paulovich, S.L. Pomeroy, T.R. Golub, E.S. Lander, and J.P. Mesirov. 2005. Gene set enrichment analysis: a knowledge-based approach for interpreting genome-wide expression profiles. *Proc. Natl. Acad. Sci. USA.* 102:15545–15550. doi:10.1073/pnas.0506580102

Vairo, G., T.J. Soos, T.M. Upton, J. Zalvide, J.A. DeCaprio, M.E. Ewen, A. Koff, and J.M. Adams. 2000. Bcl-2 retards cell cycle entry through p27(Kip1), pRB relative p130, and altered E2F regulation. *Mol. Cell. Biol.* 20:4745–4753. doi:10.1128/MCB.20.13.4745-4753.2000

Vega, R.B., B.A. Rothermel, C.J. Weinheimer, A. Kovacs, R.H. Naseem, R. Bassel-Duby, R.S. Williams, and E.N. Olson. 2003. Dual roles of modulatory calcineurin-interacting protein 1 in cardiac hypertrophy. *Proc. Natl. Acad. Sci. USA.* 100:669–674. doi:10.1073/pnas.0237225100

Wang, D., J. Feng, R. Wen, J.C. Marine, M.Y. Sangster, E. Parganas, A. Hoffmeyer, C.W. Jackson, J.L. Cleveland, P.J. Murray, and J.N. Ihle. 2000. Phospholipase Cgamma2 is essential in the functions of B cell and several Fc receptors. *Immunity.* 13:25–35. doi:10.1016/S1074-7613(00)00005-4

Whitfield, M.L., G. Sherlock, A.J. Saldanha, J.I. Murray, C.A. Ball, K.E. Alexander, J.C. Matese, C.M. Perou, M.M. Hurt, P.O. Brown, and D. Botstein. 2002. Identification of genes periodically expressed in the human cell cycle and their expression in tumors. *Mol. Biol. Cell.* 13:1977–2000.

Winslow, M.M., E.M. Gallo, J.R. Neilson, and G.R. Crabtree. 2006. The calcineurin phosphatase complex modulates immunogenic B cell responses. *Immunity.* 24:141–152. doi:10.1016/j.immuni.2005.12.013

Wu, Q., P. Kirschmeier, T. Hockenberry, T.Y. Yang, D.L. Brassard, L. Wang, T. McClanahan, S. Black, G. Rizzi, M.L. Musco, et al. 2002. Transcriptional regulation during p21WAF1/CIP1-induced apoptosis in human ovarian cancer cells. *J. Biol. Chem.* 277:36329–36337.

Xu, S., J.E. Tan, E.P. Wong, A. Manickam, S. Ponniah, and K.P. Lam. 2000. B cell development and activation defects resulting in xid-like immunodeficiency in BLNK/SLP-65-deficient mice. *Int. Immunol.* 12:397–404. doi:10.1093/intimm/12.3.397

Yanaba, K., J.D. Bouaziz, T. Matsushita, C.M. Magro, E.W. St Clair, and T.F. Tedder. 2008. B-lymphocyte contributions to human autoimmune disease. *Immunol. Rev.* 223:284–299. doi:10.1111/j.1600-065X.2008.00646.x

Yoshida, H., H. Nishina, H. Takimoto, L.E. Marengère, A.C. Wakeham, D. Bouchard, Y.Y. Kong, T. Ohteki, A. Shahinian, M. Bachmann, et al. 1998. The transcription factor NF-ATc1 regulates lymphocyte proliferation and Th2 cytokine production. *Immunity.* 8:115–124. doi:10.1016/S1074-7613(00)80464-1

Yu, D., D. Cozma, A. Park, and A. Thomas-Tikhonenko. 2005. Functional validation of genes implicated in lymphomagenesis: an in vivo selection assay using a Myc-induced B-cell tumor. *Ann. N.Y. Acad. Sci.* 1059:145–159.

Zeller, K.I., A.G. Jegga, B.J. Aronow, K.A. O'Donnell, and C.V. Dang. 2003. An integrated database of genes responsive to the Myc oncogenic transcription factor: identification of direct genomic targets. *Genome Biol.* 4:R69.